

A Dome-Headed Stem Archosaur Exemplifies Convergence among Dinosaurs and Their Distant Relatives

Michelle R. Stocker,^{1,2,7,*} Sterling J. Nesbitt,^{1,2} Katharine E. Criswell,³ William G. Parker,^{2,4} Lawrence M. Witmer,⁵ Timothy B. Rowe,⁶ Ryan Ridgely,⁵ and Matthew A. Brown^{2,6}

¹Department of Geosciences, Virginia Polytechnic Institute and State University, Blacksburg, VA 24061, USA

²Vertebrate Paleontology Laboratory, Jackson School of Geosciences, The University of Texas at Austin, J. J. Pickle Research Campus, R7600, 10100 Burnet Road, Austin, TX 78758, USA

³Department of Organismal Biology and Anatomy, University of Chicago, Chicago, IL 60637, USA

⁴Petrified Forest National Park, Petrified Forest, AZ 86028, USA

⁵Department of Biomedical Sciences, Heritage College of Osteopathic Medicine, Ohio University, Athens, OH 45701, USA

⁶Department of Geological Sciences, Jackson School of Geosciences, The University of Texas at Austin, 1 University Station, C1100, Austin, TX 78712, USA

⁷Lead Contact

*Correspondence: stockerm@vt.edu

<http://dx.doi.org/10.1016/j.cub.2016.07.066>

SUMMARY

Similarities in body plan evolution, such as wings in pterosaurs, birds, and bats or limblessness in snakes and amphisbaenians, can be recognized as classical examples of convergence among animals [1–3]. We introduce a new Triassic stem archosaur that is unexpectedly and remarkably convergent with the “dome-headed” pachycephalosaur dinosaurs that lived over 100 million years later. Surprisingly, numerous additional taxa in the same assemblage (the Otis Chalk assemblage from the Dockum Group of Texas) demonstrate the early acquisition of morphological novelties that were later convergently evolved by post-Triassic dinosaurs. As one of the most successful clades of terrestrial vertebrates, dinosaurs came to occupy an extensive morphospace throughout their diversification in the Mesozoic Era [4, 5], but their distant relatives were first to evolve many of those “dinosaurian” body plans in the Triassic Period [6–8]. Our analysis of convergence between archosauromorphs from the Triassic Period and post-Triassic archosaurs demonstrates the early and extensive exploration of morphospace captured in a single Late Triassic assemblage, and we hypothesize that many of the “novel” morphotypes interpreted to occur among archosaurs later in the Mesozoic already were in place during the initial Triassic archosauromorph, largely non-dinosaurian, radiation and only later convergently evolved in diverse dinosaurian lineages.

RESULTS AND DISCUSSION

Following the end-Permian extinctions, crown-group reptiles underwent an extensive diversification [9]. From this radiation, archosauromorphs (reptiles closer to birds and crocodylians

than to squamates) preserve one of the most diverse and disparate fossil records within Reptilia [4, 5]. The oldest and best-documented terrestrial record of this archosauromorph diversification in North America is the Late Triassic Otis Chalk assemblage [10]. This assemblage includes an exceptional range of disparate cranial morphologies, dental modifications, and overall bauplans. Common clades in this assemblage are phytosaurs, with hyper-elongated and narrow rostra that have invoked statements of convergence with extant crocodylians [7], and armored aetosaurs, resembling the Cretaceous tank-like ankylosaurian dinosaurs [8]. Reevaluation of the Otis Chalk assemblage (Supplemental Information) has illuminated further examples of convergent morphology, such as a shuvosaurid similar to *Effigia* that mimics the ornithomimid “ostrich-dinosaurs” [8, 11, 12]. Exemplifying this extreme morphological convergence, we present here a new dome-headed taxon from the assemblage, which further illustrates the extraordinary range of morphological disparity present early in the Late Triassic.

Systematic Paleontology

Reptilia Laurenti, 1768.

Archosauromorpha Huene, 1946 sensu Benton, 1985.

Archosauriformes Gauthier et al., 1988.

Triopticus primus gen. et sp. nov.

Etymology

From the Latin “tri” (three) and “optic” (vision) for the large opening in the skull roof, resembling a third eye socket. The specific name is from the Latin “primus” (first).

Holotype

Texas Vertebrate Paleontology Collections, The University of Texas at Austin (TMM) 31100-1030, posterior portion of a skull (Figures 1 and 2; Supplemental Information).

Locality and Age

Quarry 3 of the Otis Chalk localities (TMM 31100), Dockum Group, Howard County, Texas, USA. Based on biostratigraphic

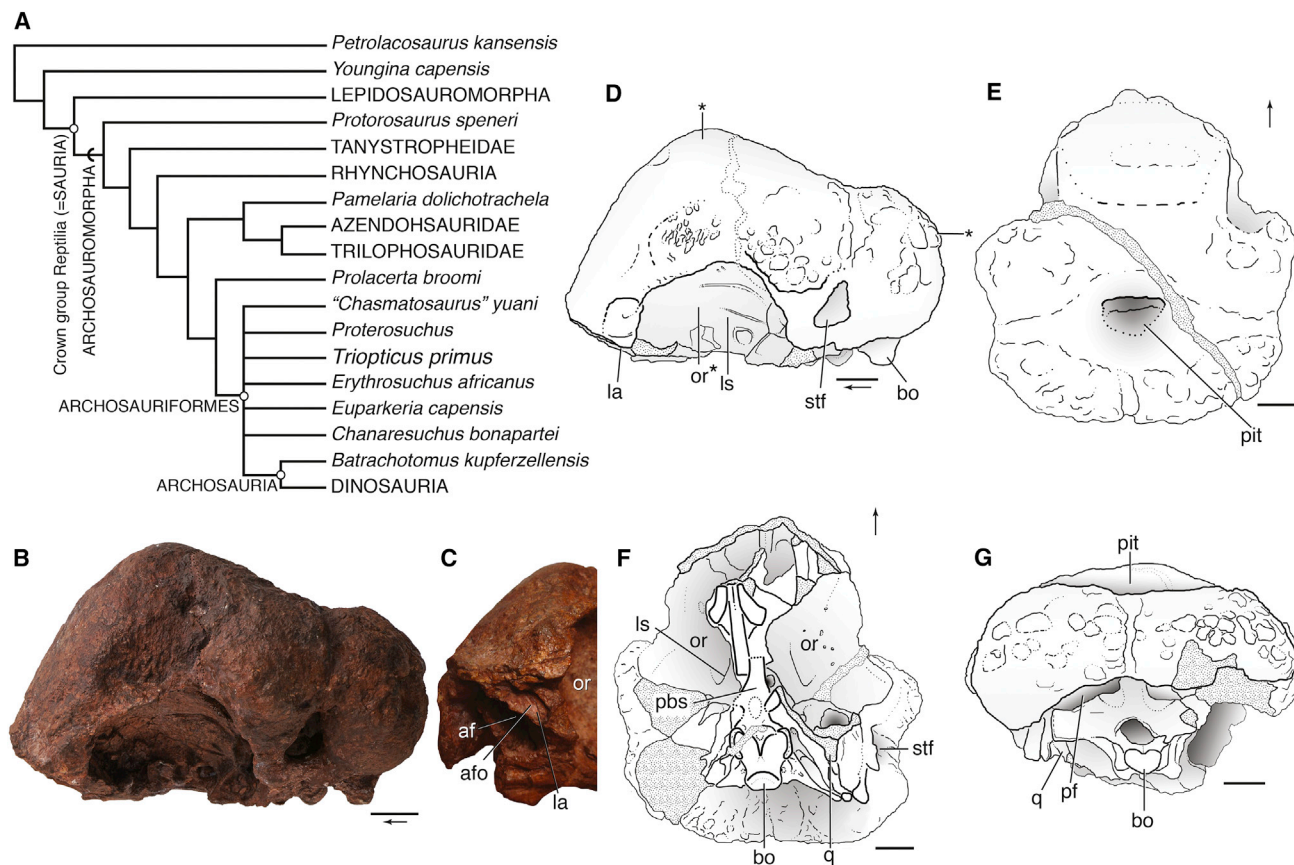


Figure 1. *Triopticus primus*, gen. et sp. nov., TMM 31100-1030

(A–G) *Triopticus* is recovered as an archosauriform within a polytomy outside of Archosauria in our phylogenetic analysis as shown in (A). The holotype specimen (TMM 31100-1030) is shown in photographs (B) and (C) and line drawing (D) in left lateral view; dorsal (E), ventral (F), and posterior (G) views illustrate the convergent morphology shared with pachycephalosaurid dinosaurs, including the posteriorly thickened and expanded posterior margin of the skull with nodes, the dorsally thickened frontal region, and the enlarged orbits (indicated by asterisks). (B) is a close-up view of the area of the antorbital fenestra and fossa. Stippled areas indicate broken surfaces or cracks in the specimen.

Abbreviations are as follows: af, antorbital fenestra; afo, antorbital fossa; bo, basioccipital; la, lacrimal; ls, laterosphenoid; or, orbit; pbs, parabasisphenoid; pf, posttemporal fenestra; pit, large median pit in skull roof; q, quadrate; stf, supratemporal fenestra. Arrows indicate anterior direction. Scale bars, 1 cm. See also Figure S1.

and lithologic correlations, the Otis Chalk localities are interpreted as Upper Triassic (latest Carnian–early Norian), ~228–220 million years (Supplemental Information).

Diagnosis

Triopticus differs from all other archosauriforms based on a unique character combination: enlarged, highly ossified cranial region of skull; enlarged orbits relative to other reptiles; fused circumorbital elements; deep pit in posterodorsal surface of skull. *Triopticus* differs from all basal dinosaurs by the presence of a horizontally oriented parabasisphenoid, broadly open posttemporal fenestrae, and a hidden squamosal-quadrate contact.

Description

The holotype braincase of *Triopticus primus* (TMM 31100-1030) is remarkable for its development of cranial excrescences or bosses that are broadly similar to those of pachycephalosaurian dinosaurs [13, 14]. The holotype individual was likely a skeletally

mature individual based on the apparent closure of nearly all sutures, as evidenced by the difficulty in tracing any clear sutures within the braincase, even in the computed tomography (CT) scan data. As a result, it is difficult to ascribe the bosses to individual bones with certainty, and thus we describe the morphology in the general anatomical regions occupied by the definitive bones. In dorsal view (see Figures 2L and 2M), five more or less discrete bosses can be identified, one of which is median (the frontal boss) and two of which are paired (the postorbital and squamosal-parietal bosses). The posterior margin of the skull, formed by the squamosal-parietal bosses, is expanded mediolaterally and posteriorly, forming a thickened shelf that overhangs and projects posteriorly well beyond the occiput; such morphology is shared with and diagnostic of Marginocephalia [15], the clade including Pachycephalosauria and Ceratopsia. As in pachycephalosaurs [14], all of the cartilages around the orbit (e.g., interorbital septum, sphenoid and ethmoid cartilages) are fully mineralized, which is extremely rare in archosauriforms.

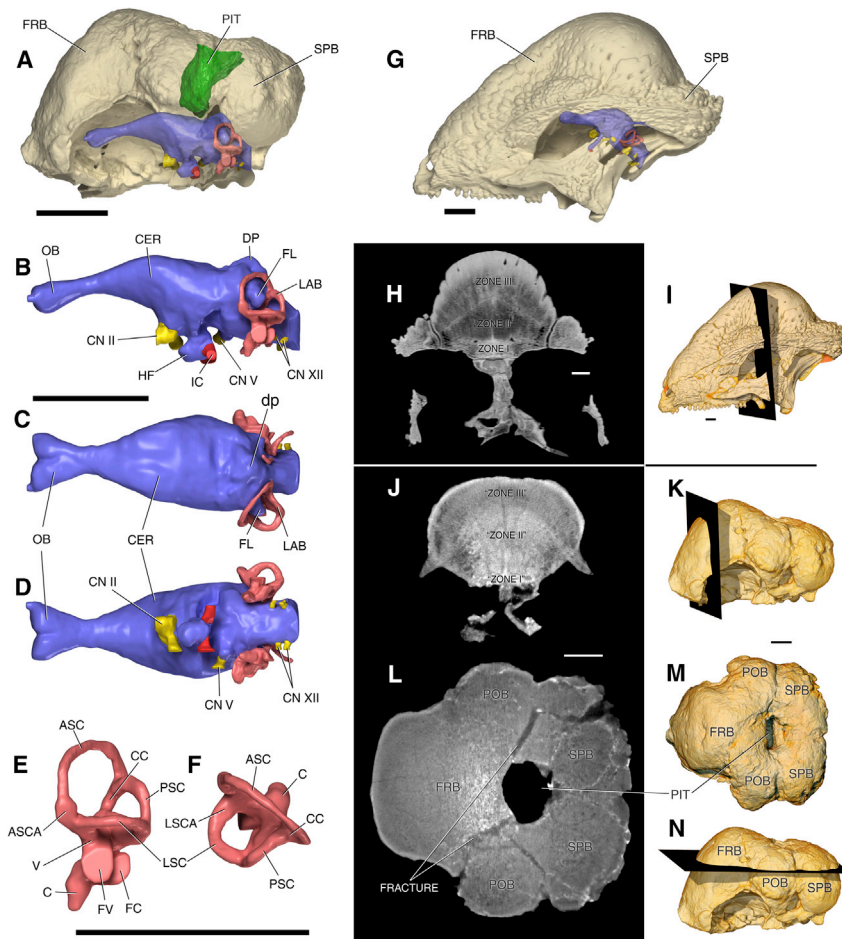


Figure 2. *Triopticus primus*, gen. et sp. nov., TMM 31100-1030

(A–N) Structure of the cranial (brain) endocast (A–F) and of the dome and bosses (A, G–N); Scale bars, 2 cm.

(A) Semitransparent braincase in left lateral view revealing the cranial (brain) endocast (blue) and the extent of the dorsal pit (green).

(B–D) Endocast of *T. primus* in left lateral (B), dorsal (C), and ventral (D) views showing the general conformation of the major brain regions, neurovasculature (yellow, red), and endosseous labyrinth (pink).

(E and F) Endosseous labyrinth of the inner ear in left lateral (E) and dorsal (F) views, showing the unexpectedly long semicircular canals, well-formed ampullae, and elongate cochlear canal.

(G) Semitransparent skull of the pachycephalosaurid *Stegoceras validum* (UALVP 2) revealing the cranial (brain) endocast (blue) and showing the overall similarity of skull form (compare with A).

(H and I) Representative axial slice (left) with an image of the skull showing the slice plane (right) of *S. validum*.

(J–N) Representative slices (left: J, axial slice; L, horizontal slice) with an image of the skull showing the slice plane (right) of *T. primus* with the exception of (M), which shows a dorsal view of the skull.

Abbreviations are as follows: ASC, anterior semicircular canal; ASCA, ampulla of ASC; C, cochlear (lagenar) canal; CC, crus communis; CER, cerebral hemisphere; CN II, cranial nerve II (optic n.); CN V, cranial nerve V (trigeminal n.); CN XII, cranial nerve XII (hypoglossal n.); DP, dural peak; FC, fenestra cochleae (foramen metoticum); FL, cerebellar flocculus; FRB, frontal boss; FV, fenestra vestibuli (ovalis); HF, hypophyseal (pituitary) fossa;

IC, internal carotid artery canal; LAB, endosseous labyrinth; LSC, lateral semicircular canal; LSCA, ampulla of LSC; OB, olfactory bulb; POB, postorbital boss; PSC, posterior semicircular canal; SPB, squamosal-parietal boss; V, vestibule. Scale bars, 1 cm. See also [Figure S1](#).

In all cases, the surfaces of the bosses show dermal sculpture that is highly roughened, presumably reflective of hypermineralization (i.e., calcification and/or deposition of bone minerals such as hydroxyapatite in tissues that are not typically mineralized in related species) and ultimately ossification of the dermis, as in a variety of other archosaurs [16, 17]. Thus, it is likely that these bosses were covered in some kind of tough keratinized epidermal covering, although the exact form of the integumentary covering is unknown. All five bosses surround a curious large, approximately 2 cm-deep, median pit, the nominative attribute of *Triopticus*. The fact that the surrounding surface-bone ornamentation continues into the pit suggests that the walls of the pit likewise were covered with integument. Its most likely interpretation is as an epiphenomenon resulting from expansion of the surrounding paired bosses noted above (much like the hole of a doughnut). Another less likely but still viable hypothesis is that the pit is a pineal foramen (Figure 1D), although this character state is not present otherwise in Archosauriformes [18] (Supplemental Information).

The internal structure of the bosses shows potential “zonation” of bone microstructure, perhaps suggesting that the observed convergence with pachycephalosaurs is literally “more

than skin deep.” Goodwin and Horner [19] noted that in pachycephalosaurs, the histological structure of the dome can be partitioned into three zones: zone I is deepest and largely resembles normal skull roofing bones, zone II is intermediate in depth and is porous and vascular, and zone III is most superficial and less vascular. Evans et al. [13] identified these same three zones based on CT scan data, and we show (Figure 2H) the zonation in our own CT scan data of the pachycephalosaurid *Stegoceras validum* (UALVP 2). *Triopticus* can also be interpreted as having a similar kind of three-part zonation (Figures 2J and 2L). The deepest layer (“zone I”) clearly pertains to the typical skull roofing elements. “Zone II” and “zone III” also are clearly visible as distinct zones and are consistent throughout at least the frontal boss region, as evidenced by an axial slice (Figure 2J). Zone II also is very porous, and enough of the pore spaces could be traced to show continuity consistent with a vascular interpretation, although general cancellous structure cannot be ruled out in some areas. It may be relevant here that Goodwin and Horner [19] noted that vascular porosity decreases as pachycephalosaurs age, and, as stated above, the holotype specimen of *Triopticus* apparently is from a skeletally mature individual. We do not want to make more of the similarity than is merited; the structure

is not identical. For example, in pachycephalosaurs, zone II is less dense than zone III [13, 19], whereas the reverse is true in *Triopticus*, although this difference could relate not to biological density (e.g., vascular porosity) but rather to radiological density and the diagenetic deposition of radiodense minerals. Caveats notwithstanding, the possibility remains that evolutionary convergence in gross dome and/or boss structure may also carry over to histological structure, and this hypothesis could be tested with additional finds of *Triopticus*.

Anteriorly on the lacrimal, a narrow area of smooth bone with a finished anteroventral edge forms an antorbital fossa and fenestra, a critical character state that clearly places *Triopticus* within Archosauriformes [18] (see phylogenetic analysis in [Supplemental Information](#)). Posteriorly, the articulated left quadrate head is angled anteroventrally, implying the presence of a jaw joint anterior to the posterior margin of the skull as in, but not exclusive to, pachycephalosaurids [14].

From CT scan data ([Figure 2](#); [Supplemental Information](#)), the digital cranial endocast reveals an overall structure of the brain and inner ear labyrinth that largely is consistent with that of other basal archosauriforms, although the semicircular canals are surprisingly elongate and the floccular lobe of the cerebellum is unexpectedly large. The endocast is superficially similar to that of the pachycephalosaur *Stegoceras* in structure and proportions, but that similarity can largely be attributed to generally plesiomorphic brain organization, coupled with hypermineralization of the surrounding cartilages and dermis associated with the braincase.

The Triassic Period, as exemplified by the Otis Chalk assemblage, was a time of bauplan experimentation among archosauriforms, showing high disparity in the Late Triassic [20, 21]. Disparate cranial morphotypes include (1) elongated, possibly piscivorous-adapted rostra such as in proterochampsids and doswelliids, taken to the extreme of hyper-elongation in phytosaurs; (2) carnivorous and hypercarnivorous morphotypes like those of erythrosuchids, rauisuchids, and early dinosaurs; (3) “herbivorous” taxa with leaf-shaped teeth such as *Azendohsaurus*, aetosaurs, *Revueltosaurus*, and silesaurids; and (4) beaked taxa like shuvosaurids. However, these different morphotypes do not characterize monophyletic clades but rather reflect phylogenetic constraint from common ancestry [22] and within-Triassic morphological convergence across distantly related clades [5, 18, 23], which highlights this time period as one of remarkable experimentation.

Dinosaurs and crocodylomorphs, the archosauriforms that survived the end-Triassic extinction, in a sense, independently re-evolved morphological suites that first arose in the Triassic [4, 6–8, 24, 25]. Many of these recurring morphologies are found in post-Triassic ornithomimosaurs, such as sauropodomorphs, ornithomimosaurs, and spinosaurid dinosaurs, but especially within Ornithischia, including thyreophorans (e.g., *Scutellosaurus*, ankylosaurs) and, as we demonstrate here, between *Triopticus* and Cretaceous pachycephalosaurs. These disparate morphotypes appear to be part of an iterative pattern of morphological evolution, where Triassic archosauriforms occupied adaptive zones that dinosaurs filled later in the Mesozoic after the end-Triassic extinction of most non-dinosaurian and non-crocodyliform archosauriforms. For example, the elongate rostra of phytosaurs are repeated in spinosaurids (Theropoda) and also

in extant crocodylians (Crocodylia); leaf-shaped teeth appear in ornithischians, therizinosaurs (Theropoda), and even some crocodyliforms [26]; and beaks are known in ornithomimosaurs, oviraptorosaurs, and Aves (Theropoda).

Previously, these similarities only have been discussed superficially and anecdotally (e.g., [6, 8, 11]). Therefore, to provide a quantitative examination of this morphological convergence across the Mesozoic, we analyzed an independent morphological character dataset, focused on examining the overlap of morphospace within a phylogenetic context (through previous, independent phylogenetic analyses; [Supplemental Information](#)) rather than highlighting rates of morphological character change or inferences of competitive succession. Moreover, this novel analysis is presented in a testable framework using non-metric multidimensional scaling (nMDS; [Supplemental Information](#)). Our morphological characters cover the full skeleton as well as indicate some functional interpretations (i.e., quadrupedal versus bipedal). We focused our choice of Triassic taxa on those found in the diverse Late Triassic Otis Chalk faunal assemblage in comparison with convergent post-Triassic taxa. We included archosauriforms with a “plesiomorphic” bauplan to test whether the morphological convergence among these Triassic and post-Triassic taxa is the result of common ancestry or convergence.

Compared with our post-Triassic archosaur taxa, the Triassic archosauriform taxa included in our analysis of skeletal ([Figure 3A](#)) and cranial ([Figure 3B](#)) morphospace indicate an extensive Triassic coverage of archosauriform morphospace ([Figure 3C](#)). Clusters of taxa reflect (1) a central grouping of various plesiomorphic archosauriform bauplans (i.e., *Euparkeria*, *Prolacerta*, *Protorosaurus*, *Protosuchus*); (2) convergent bauplans among Triassic archosauriforms and post-Triassic archosaurs (e.g., long-snouted, armored, bipedal carnivorous, beaked, and dome-headed taxa). Analyzing only cranial characters, some groupings such as long-snouted taxa become more closely associated but are slightly separated in the complete bauplan analysis because they retain more plesiomorphic postcrania.

A prime point from our analysis is the lack of temporal overlap of each Triassic and post-Triassic morphotype ([Figure 4](#)). The various sets of convergent taxa examined here are separated by ranges of a few tens of millions of years (e.g., *Angistorhinus* and *Pelagosaurus*) to over 100 million years in the case of *Triopticus* and *Stegoceras*. Moreover, the similar body plans of *Effigia*, *Limusaurus*, and *Ornithomimus* occur without temporal overlap spanning 150 million years. In the Otis Chalk assemblage, these early archosauriform bauplans are present in a single time and locality, whereas post-Triassic representatives of these bauplans are spread across both time and space, never accumulating in one assemblage.

From our analyses, the archosauriform radiation, which includes early dinosaurs, appears to show in the Triassic a near saturation of most archosauriform morphospace for the Mesozoic. However, those Triassic archosauriforms do not represent all subsequent archosaur bauplans, specifically those of ceratopsians, gigantic sauropodomorphs, and maniraptoran theropods. These dinosaurian morphotypes are unique across animals, having no convergent morphotype in the Phanerozoic. Similar patterns of early morphospace occupation, extinctions,

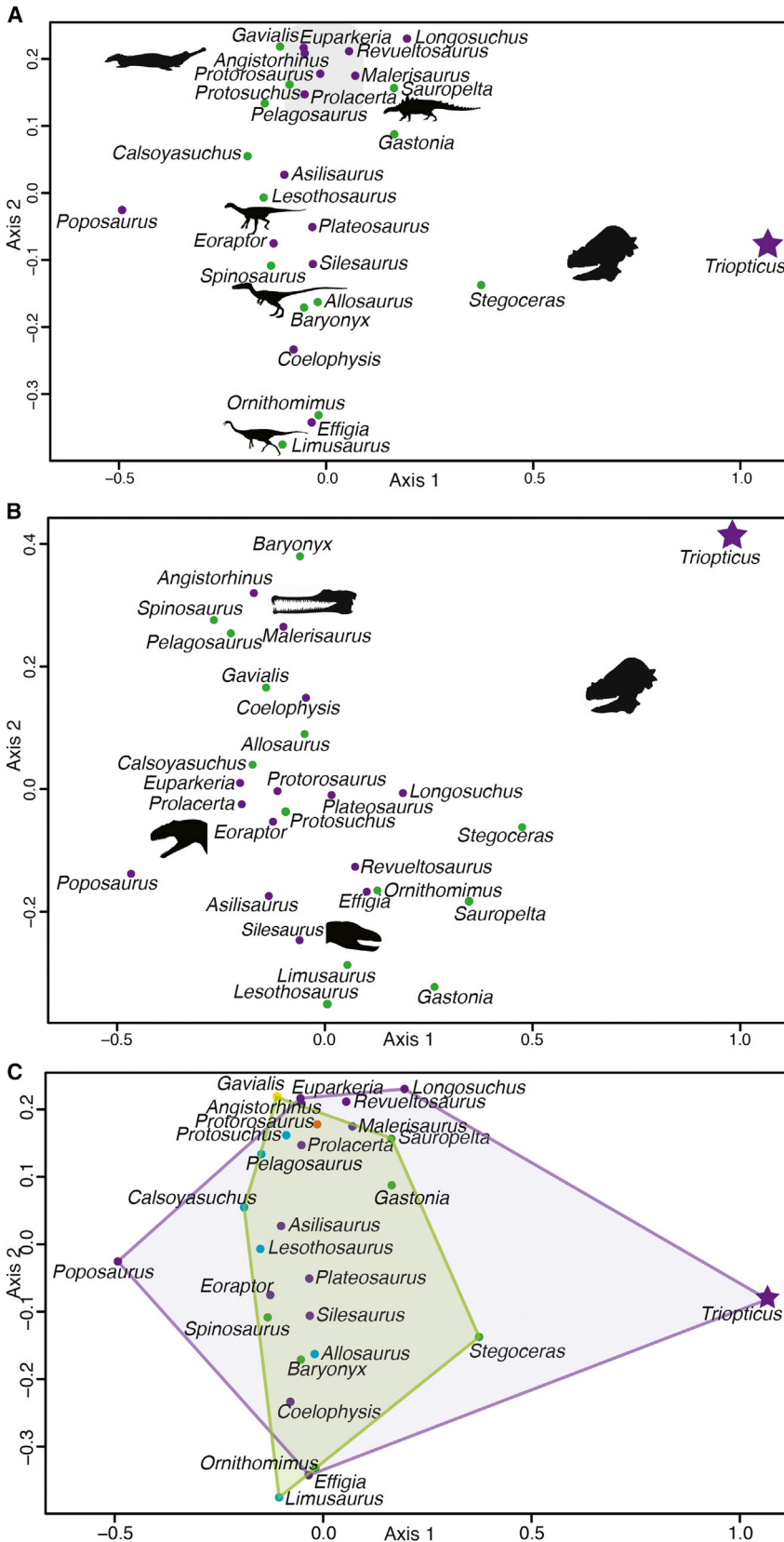


Figure 3. nMDS Plots Depicting Convergence of Post-Triassic Archosaurs on the Morphologies and Body Plans of Triassic Archosauromorphs

(A) Plot of overall bauplan convergence, using all characters (cranial and postcranial). Gray cloud indicates plesiomorphic bauplan.

(B) Plot of cranial character convergence only. Here, we find a grouping of long-snouted taxa in the upper left, a plesiomorphic, carnivorous grouping in the middle left, and a large herbivorous grouping in the bottom center.

(C) Same plot as (A), showing overlap of Triassic (purple polygon) with post-Triassic (green polygon) taxa.

Dot colors represent time periods for each taxon: orange = Permian; purple = Triassic; green = Jurassic; blue = Cretaceous; yellow = Quaternary. Axes represent distance scores according to the Gower distance metric used in the nMDS analysis. See also [Figures S2–S4](#) and [Tables S1–S3](#). Silhouettes through Phylopic, courtesy of Scott Hartman and Emily Willoughby.

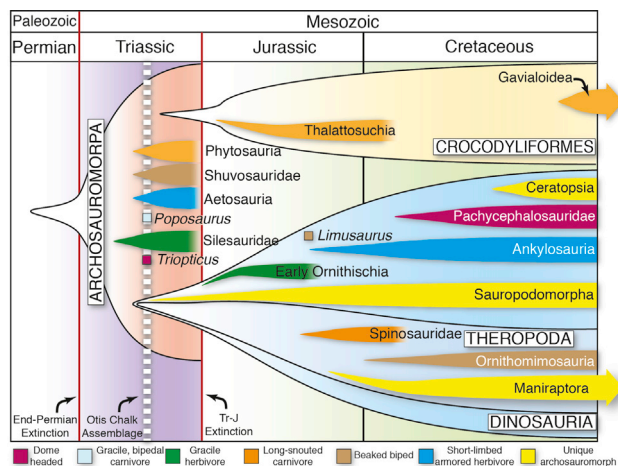


Figure 4. The Overall Convergence of Skeletal Bauplans among Triassic Archosauromorpha and Post-Triassic Crocodyliform and Dinosaur Groups, as Illustrated through the Mesozoic

The morphologies of many of the members of the Late Triassic Otis Chalk assemblage (indicated by white, dashed vertical line) are later repeated by many dinosaur groups temporally separated by the end-Triassic mass extinction. See also Figure S2.

and the convergent replacement of that morphospace have been proposed for Ediacara species [27], early Paleozoic crinoids [28], Late Cretaceous and early Paleogene reef fishes [29], and several other groups [30, 31], and each of these events may be reflective of deep constraints in both morphological evolution and in how environments transition to apparent ecological stability after mass extinctions (e.g., [32, 33]). Whereas the end-Permian extinction began the process of iterative evolution of disparate archosauromorph morphotypes, the end-Triassic extinction of most non-dinosaurian archosauriforms may have provided opportunities for the surviving archosaurs to repeat that process of bauplan experimentation radiating into Triassic ecomorphologies during the later portions of the Phanerozoic.

EXPERIMENTAL PROCEDURES

Preparation Methods

The specimen was preserved in a red mudstone and covered in a ~1 mm thick hematite rind. Gross mechanical preparation began with water, toothbrush, and carbide needle in pin vise to remove the mudstone; fine preparation continued with carbide needles in pin vise and an HW-10 airscribe. All mechanical preparation was under a Wild M8 binocular microscope. Preparation of the rugose dorsal surface of the skull was supplemented chemically with a 10% solution of acetic acid buffered with tri-basic calcium phosphate. Paraloid B-72 (Rohm and Haas) was used as an acid barrier, and Paleobond PB40 cyanoacrylate (Uncommon Conglomerates) was used to consolidate small cracks. Paraloid B-72 was used as a release agent, and Carbowax 1000 grade polyethylene glycol (Dow Chemical) was used as a gap filler. The skull was molded using Platsil 73-25 (Polytek) platinum silicone rubber.

CT Methods

Scanning was performed by Matthew Colbert at UTCT as Archive 2385 on December 10, 2010 with 200 kV and 0.3 mA. Slice thicknesses were 0.0853 mm, with an inter-slice spacing of 0.0853 mm, and field of reconstruction at 81 mm. Final resolution was 1024 × 1024 pixels and 16-bit grayscale. Post-processing visualizations can be freely accessed online through MorphoSource under project P181 (<http://morphosource.org/index.php>).

Phylogenetic Methods

We analyzed the phylogenetic relationships of *Triopticus primus* using a modified version of the matrix of [23] for *Azendohsaurus madagaskarensis* (see Supplemental Information for further details).

Disparity Analysis Methods

We quantified the apparent convergent morphologies of Late Triassic archosauromorphs and post-Triassic archosauromorphs using an ordination analysis (nMDS) performed in the R software packages Claddis [34] and vegan [35] on a morphological character matrix developed independently of the matrix used for the phylogenetic analysis. This matrix included a wide range of morphological features associated with specialized ecomorphologies that have been cited as convergently evolved between non-dinosaurian archosaurs and dinosaurs (e.g., [8, 24]). We converted our character-taxon matrix of 28 taxa and 81 morphological characters into a distance matrix in Claddis [34], which uses a combination of the Gower and generalized Euclidean distances, and ran an nMDS analysis using the metaMDS command in vegan [35] with four dimensions and a maximum of 1,000 random starts. See Supplemental Information for extended explanation of methods.

SUPPLEMENTAL INFORMATION

Supplemental Information includes Supplemental Experimental Procedures, four figures, and three tables and can be found with this article online at <http://dx.doi.org/10.1016/j.cub.2016.07.066>.

AUTHOR CONTRIBUTIONS

M.R.S., S.J.N., K.E.C., W.G.P., and T.B.R. designed the research project. M.A.B. prepared the specimen. M.R.S., K.E.C., L.M.W., and R.R. interpreted CT data. M.R.S., S.J.N., and K.E.C. described the specimen. M.R.S. and S.J.N. conducted the phylogenetic analysis. M.R.S., S.J.N., and K.E.C. conducted the disparity analyses. M.R.S., S.J.N., K.E.C., W.G.P., L.M.W., and M.A.B. wrote the manuscript.

ACKNOWLEDGMENTS

We thank M. Colbert for CT scanning *Triopticus primus*. J.C. Sagebiel provided access to comparative material. Discussion with A. Pritchard clarified comparisons with other archosauromorph taxa, and D. Evans, J. Horner, and M. Goodwin offered knowledge of pachycephalosaur dinosaurs. Discussion with H. O'Brien clarified statistical methods and interpretations. M. Coates and P. Olsen provided useful comments, as did our three reviewers. Support for this work was provided in part by the John A. and Katherine G. Jackson School of Geosciences and the Geology Foundation at the University of Texas at Austin.

Received: June 7, 2016

Revised: July 23, 2016

Accepted: July 26, 2016

Published: September 22, 2016

REFERENCES

- Lee, M.S.Y. (1998). Convergent evolution and character correlation in burrowing reptiles: towards a resolution of squamate relationships. *Biol. J. Linn. Soc. Lond.* 65, 369–453.
- McGhee, G.R., Jr. (2011). *Convergent Evolution: Limited Forms Most Beautiful* (Cambridge: MIT Press).
- Osborn, H.F. (1905). The ideas and terms of modern philosophical anatomy. *Science* 27, 959–961.
- Brusatte, S.L., Benton, M.J., Ruta, M., and Lloyd, G.T. (2008). The first 50 Myr of dinosaur evolution: macroevolutionary pattern and morphological disparity. *Biol. Lett.* 4, 733–736.
- Brusatte, S.L., Nesbitt, S.J., Irmis, R.B., Butler, R.J., Benton, M.J., and Norell, M.A. (2010). The origin and early radiation of dinosaurs. *Earth Sci. Rev.* 101, 68–100.

6. Chatterjee, S. (1985). *Postosuchus*, a new thecodontian reptile from the Triassic of Texas and the origin of tyrannosaurs. *Philos. Trans. R. Soc. Lond. B Biol. Sci.* 309, 395–460.
7. Hunt, A.P. (1989). Cranial morphology and ecology among phytosaurs. In *Dawn of the Age of Dinosaurs in the American Southwest*, S.G. Lucas, and A.P. Hunt, eds. (Albuquerque: New Mexico Museum of Natural History), pp. 349–354.
8. Nesbitt, S.J., and Norell, M.A. (2006). Extreme convergence in the body plans of an early suchian (Archosauria) and ornithomimid dinosaurs (Theropoda). *Proc. Biol. Sci.* 273, 1045–1048.
9. Benton, M.J. (1995). Diversification and extinction in the history of life. *Science* 268, 52–58.
10. Long, R.A., and Murry, P.A. (1995). Late Triassic (Carnian and Norian) tetrapods from the southwestern United States. *New Mexico Museum of Natural History & Science Bulletin* 4, 1–254.
11. Chatterjee, S. (1993). *Shuvosaurus*, a new theropod. *National Geographic Research & Exploration* 9, 274–285.
12. Nesbitt, S.J. (2007). The anatomy of *Effigia okeeffeae* (Archosauria, Suchia), theropod-like convergence, and the distribution of related taxa. *Bull. Am. Mus. Nat. Hist.* 302, 1–84.
13. Evans, D.C., Schott, R.K., Larson, D.W., Brown, C.M., and Ryan, M.J. (2013). The oldest North American pachycephalosaurid and the hidden diversity of small-bodied ornithischian dinosaurs. *Nat. Commun.* 4, 1828.
14. Maryańska, T., Chapman, R.E., and Weishampel, D.B. (2004). Pachycephalosauria. In *The Dinosauria*, Second Edition, D.B. Weishampel, P. Dodson, and H. Osmólska, eds. (Berkeley: University of California Press), pp. 464–477.
15. Sereno, P.C. (1986). Phylogeny of the bird-hipped dinosaurs (Order Ornithischia). *Natl. Geogr. Res.* 2, 234–256.
16. Hieronymus, T.L., Witmer, L.M., Tanke, D.H., and Currie, P.J. (2009). The facial integument of centrosaurine ceratopsids: morphological and histological correlates of novel skin structures. *Anat. Rec. (Hoboken)* 292, 1370–1396.
17. Sampson, S.D., and Witmer, L.M. (2007). Craniofacial anatomy of *Majungasaurus crenatissimus* (Theropoda: Abelisauridae) from the Late Cretaceous of Madagascar. *Memoirs of the Society of Vertebrate Paleontology* 8. *J. Vertebr. Paleontol.* 27, 32–102.
18. Nesbitt, S.J. (2011). The early evolution of archosaurs: relationships and the origin of major clades. *Bull. Am. Mus. Nat. Hist.* 352, 1–292.
19. Goodwin, M.B., and Horner, J.R. (2004). Cranial histology of pachycephalosaurs (Ornithischia: Marginocephalia) reveals transitory structures inconsistent with head-butting behavior. *Paleobiology* 30, 253–267.
20. Fraser, N. (2006). *Dawn of the Dinosaurs: Life in the Triassic* (Bloomington: Indiana University Press).
21. Sues, H.-D., and Fraser, N.C. (2010). *Triassic Life on Land: The Great Transition* (New York: Columbia University Press).
22. McKittrick, M.C. (1993). Phylogenetic constraint in evolutionary theory; has it any explanatory power? *Annu. Rev. Ecol. Syst.* 24, 307–330.
23. Nesbitt, S.J., Flynn, J.J., Pritchard, A.C., Parrish, J.M., Ranivoharimanana, L., and Wyss, A.R. (2015). Postcranial osteology of *Azendohsaurus madagaskarensis* (?Middle to Upper Triassic, Isalo Group, Madagascar) and its systematic position among stem archosaur reptiles. *Bull. Am. Mus. Nat. Hist.* 899, 1–125.
24. Flynn, J.J., Nesbitt, S.J., Parrish, J.M., Ranivoharimanana, L., and Wyss, A.R. (2010). A new species of *Azendohsaurus* (Diapsida: Archosauromorpha) from the Triassic Isalo Group of southwestern Madagascar: cranium and mandible. *Palaeontology* 53, 669–688.
25. Sill, W.D. (1974). The anatomy of *Saurosuchus galilei* and the relationships of the rauisuchid thecodonts. *Bull. Mus. Comp. Zool.* 146, 317–362.
26. Kley, N.J., Sertich, J.J.W., Turner, A.H., Krause, D.W., O'Connor, P.M., and Georgi, J.A. (2010). Craniofacial morphology of *Simosuchus clarki* (Crocodyliformes: Notosuchia) from the Late Cretaceous of Madagascar. *Society of Vertebrate Paleontology Memoir* 10. *J. Vertebr. Paleontol.* 30, 13–98.
27. Shen, B., Dong, L., Xiao, S., and Kowalewski, M. (2008). The Avalon explosion: evolution of Ediacara morphospace. *Science* 319, 81–84.
28. Foote, M. (1994). Morphological disparity in Ordovician-Devonian crinoids and the early saturation of morphological space. *Paleobiology* 20, 320–344.
29. Price, S.A., Schmitz, L., Oufiero, C.E., Eytan, R.I., Dornburg, A., Smith, W.L., Friedman, M., Near, T.J., and Wainwright, P.C. (2014). Two waves of colonization straddling the K-Pg boundary formed the modern reef fish fauna. *Proc. Biol. Sci.* 281, 20140321.
30. Hughes, M., Gerber, S., and Wills, M.A. (2013). Clades reach highest morphological disparity early in their evolution. *Proc. Natl. Acad. Sci. USA* 110, 13875–13879.
31. Benton, M.J., Forth, J., and Langer, M.C. (2014). Models for the rise of the dinosaurs. *Curr. Biol.* 24, R87–R95.
32. Roopnarine, P.D., and Angielczyk, K.D. (2015). Community stability and selective extinction during the Permian-Triassic mass extinction. *Science* 350, 90–93.
33. Ruta, M., Angielczyk, K.D., Fröbisch, J., and Benton, M.J. (2013). Decoupling of morphological disparity and taxic diversity during the adaptive radiation of anomodont therapsids. *Proc. Biol. Sci.* 280, 20131071.
34. Lloyd, G.T. (2015). Claddis: an R package for performing disparity and rate analysis on cladistic-type data sets. <https://github.com/graemetlloyd/Claddis>.
35. Oksanen, J., Blanchet, F.G., Kindt, R., Legendre, P., Minchin, P.R., O'Hara, R.B., Simpson, G.L., Solymos, P., Stevens, M.H.H., and Wagner, H. (2015). *vegan: Community Ecology Package*. R package version 2.3-0. <http://CRAN.R-project.org/package=vegan>.

Current Biology, Volume 26

Supplemental Information

A Dome-Headed Stem Archosaur

Exemplifies Convergence among Dinosaurs

and Their Distant Relatives

Michelle R. Stocker, Sterling J. Nesbitt, Katharine E. Criswell, William G. Parker, Lawrence M. Witmer, Timothy B. Rowe, Ryan Ridgely, and Matthew A. Brown

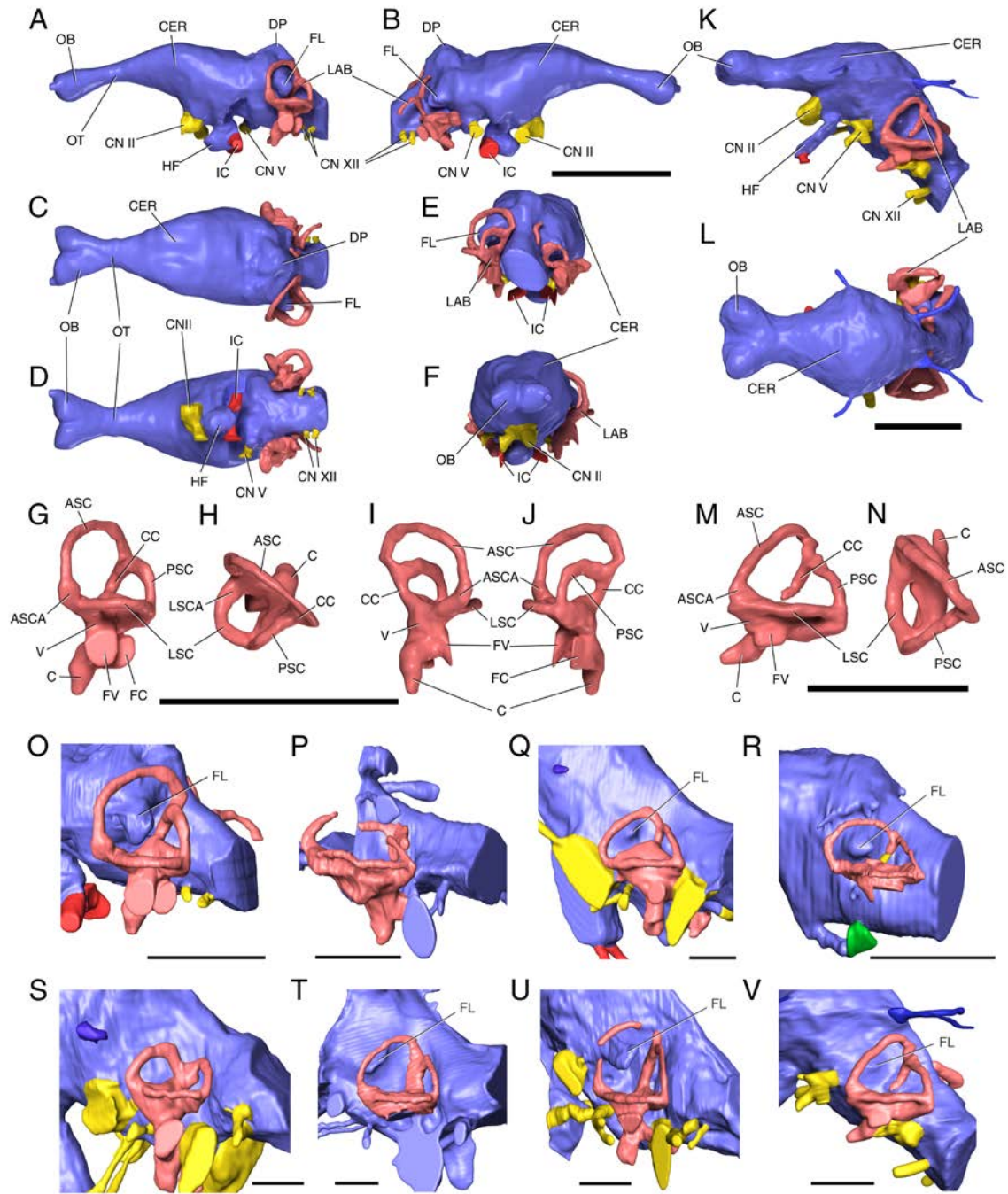


Figure S1: *Triopticus primus*, gen. et sp. nov. (TMM 31100-1030). Related to Figures 1 and 2. **A-F**, Cranial (brain) endocast in **A**, left lateral, **B**, right lateral, **C**, dorsal, **D**, ventral, **E**, posterior, and **F**, anterior views. **G-J**, Left endosseous labyrinth in **G**, lateral, **H**, dorsal, **I**, anterior, and **J**, posterior views. **K-N**, *Stegoceras validum* (UALVP 2, reversed), cranial endocast in **K**, left lateral and **L**, dorsal views, and left endosseous labyrinth in **M**, lateral and **N**, dorsal views. **A-N**, Scale bars = 2 cm. **O-V**, Comparison of the posterior regions of the cranial endocast and endosseous labyrinth, highlighting the presence or absence of the cerebellar flocculus as well as the structure of the labyrinth (in pink). All in left posterolateral view. Scale bars = 1 cm. **O**, *Triopticus primus*, gen. et sp. nov. (TMM 31100-1030). **P**, *Chanaresuchus bonapartei* (MCZ 4037). Note that the endocast is incomplete, but that there is no indication that a flocculus was present. **Q**, *Parasuchus hislopi* (ISI R44). **R**, *Gracilisuchus stipanicorum* (MCZ 4117);

reversed). **S**, *Desmotosuchus spurensis* (UCMP 27410). **T**, *Postosuchus* sp. cf. *P. kirkpatricki* (UMMP 7473). **U**, *Herrerasaurus ischigualastensis* (MCZ 7063; reversed). **V**, *Stegoceras validum* (UALVP 2; reversed). Abbreviations: ASC, anterior semicircular canal; ASCA, ampulla of ASC; C, cochlear (lagenar) canal; CC, crus communis; CER, cerebral hemisphere; CN II, cranial nerve II (optic n.); CN V, cranial nerve V (trigeminal n.); CN XII, cranial nerve XII (hypoglossal n.); DP, dural peak; FC, fenestra cochleae (foramen metoticum); FL, cerebellar flocculus; FV, fenestra vestibuli (ovalis); HF, hypophyseal (pituitary) fossa; IC, internal carotid artery canal; LAB, endosseous labyrinth; LSC, lateral semicircular canal; LSCA, ampulla of LSC; OB, olfactory bulb; OT, olfactory tract; PSC, posterior semicircular canal; V, vestibule.

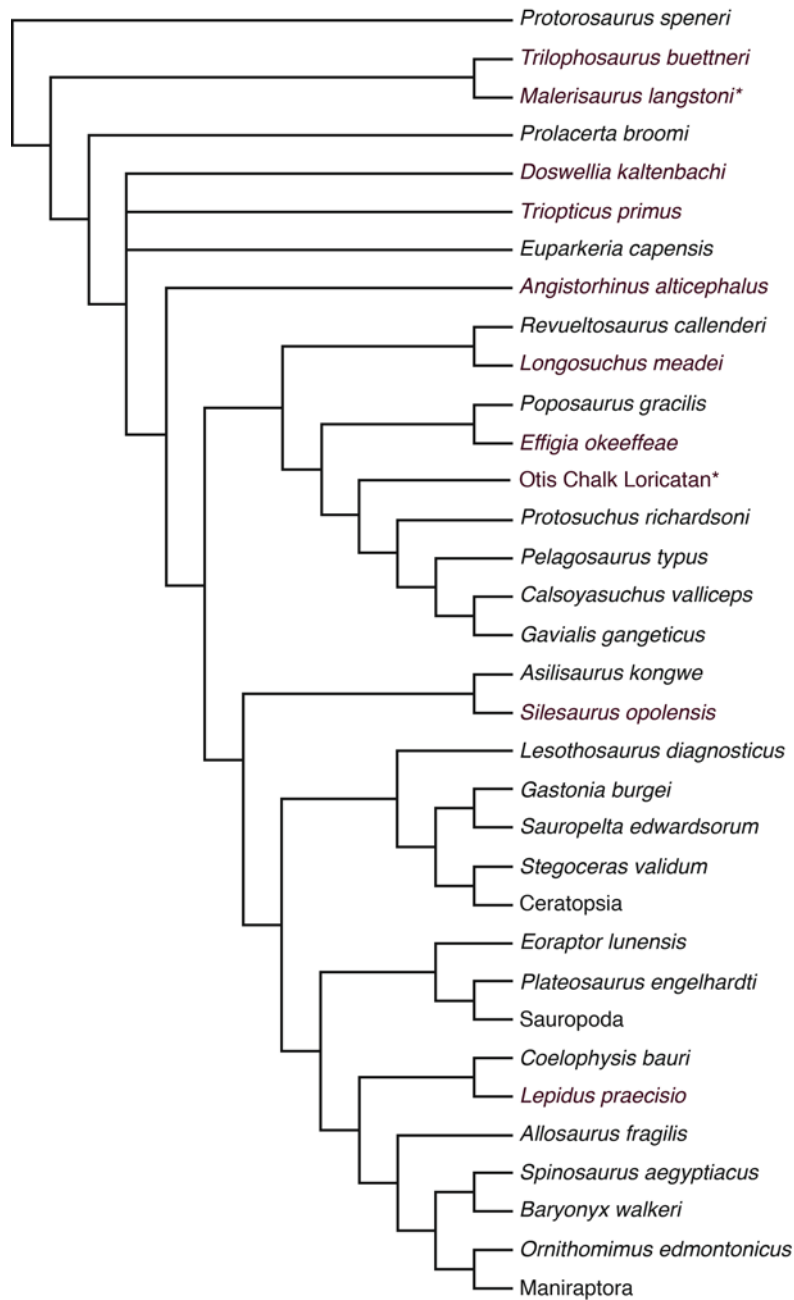


Figure S2: Phylogenetic tree of all taxa included in convergence analysis, related to Figures 3 and 4. Phylogeny assembled from the following sources: [S1-10]. Taxon names in purple are those from the Otis Chalk assemblage. The phylogenetic positions of taxa with an asterisk (*) are resolved here based on unpublished data.

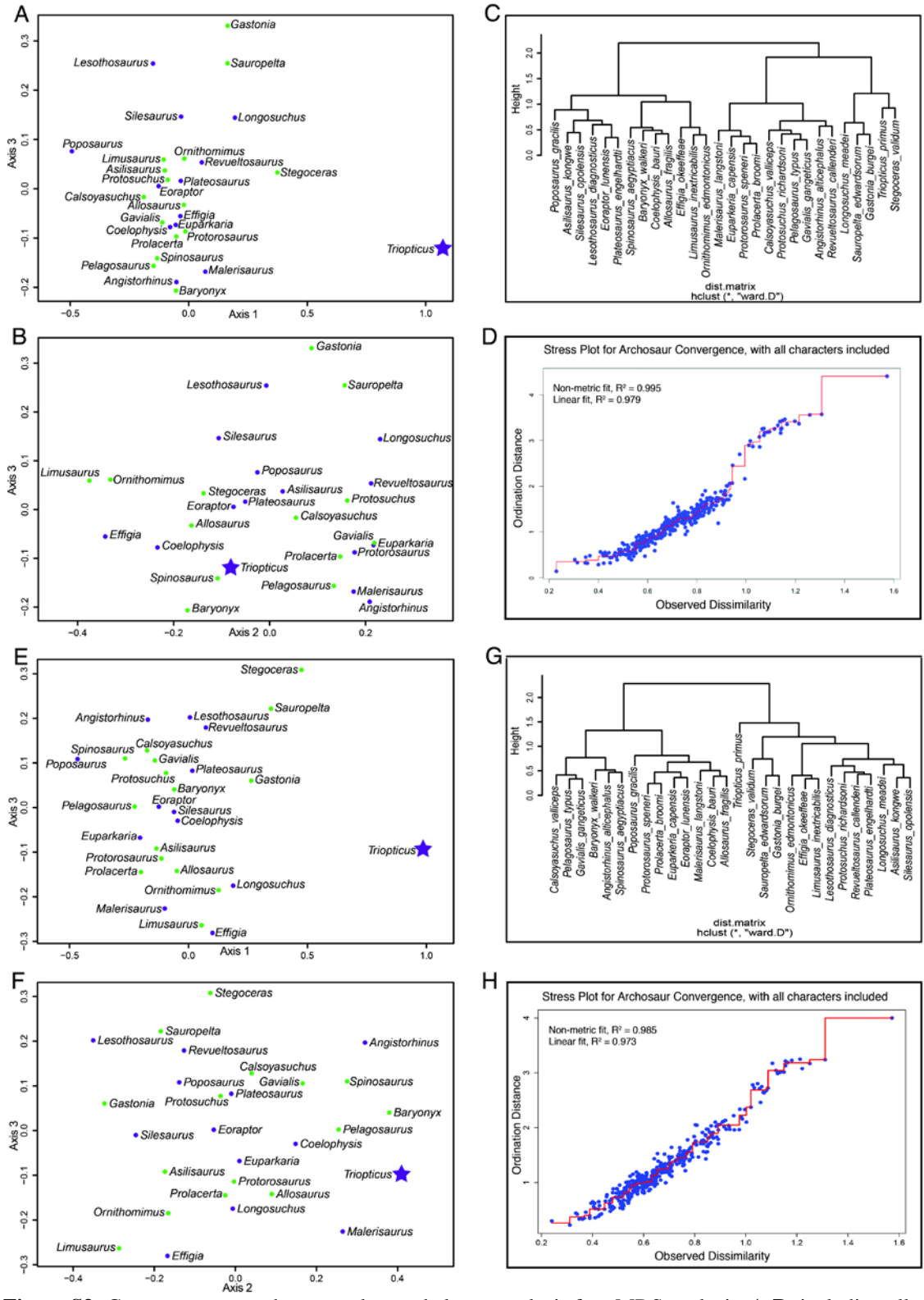


Figure S3: Convergence morphospace plots and cluster analysis for nMDS analysis. **A-D**, including all characters and stress plot for nMDS analysis using both cranial and postcranial characters, and **E-H**, for nMDS analysis including only cranial characters and stress plot for nMDS analysis using only cranial characters. Related to Figure 3. **A**, axis 1 plotted against axis 3. **B**, axis 2 plotted against axis 3. Purple dots

represent Triassic taxa, with a purple star indicating the position of *Triopticus*, and green dots represent post-Triassic taxa. **C**, cluster analysis of all taxa included in this nMDS analysis. **D**, stress plot for analysis including all characters. **E**, axis 1 plotted against axis 3. **F**, axis 2 plotted against axis 3. Purple dots represent Triassic taxa, with a purple star indicating the position of *Triopticus*, and green dots represent post-Triassic taxa. **G**, cluster analysis of all taxa included in this nMDS analysis. **H**, stress plot for analysis using only cranial characters.

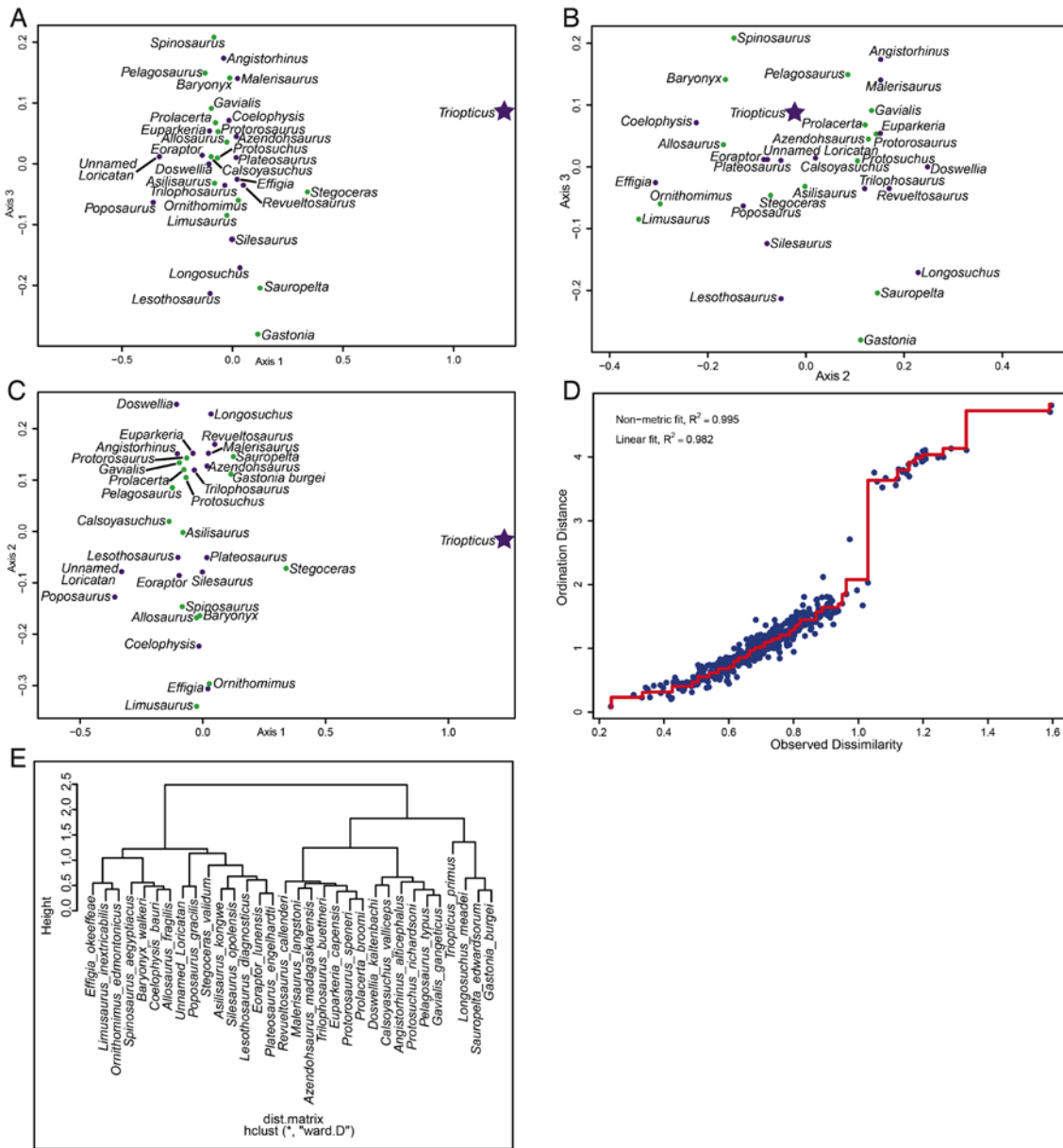


Figure S4: Convergence morphospace plots, stress plot, and cluster analysis for nMDS analysis including all taxa from the Otis Chalk assemblage, and both postcranial and cranial characters, related to Figure 3. **A**, axis 1 plotted against axis 3. **B**, axis 2 plotted against axis 3. **C**, axis 1 plotted against axis 2. Purple dots represent Triassic taxa, with a purple star indicating the position of *Triopticus*, and green dots represent post-Triassic taxa. **D**, stress plot for nMDS analysis. **E**, cluster analysis of all taxa included in this nMDS analysis.

Table S1: Convergence scores for the nMDS analysis using both cranial and postcranial characters, related to Figure 3.

	NMDS1	NMDS2	NMDS3	NMDS4
<i>Protorosaurus_speneri</i>	-0.012782601	0.177515433	0.086273503	0.171546724
<i>Malerisaurus_langstoni</i>	0.071319301	0.174198278	0.167177737	0.045048434
<i>Prolacerta_broomi</i>	-0.050885345	0.147042635	0.097254382	0.167056082
<i>Angistorhinus_alticephalus</i>	-0.049892588	0.208255888	0.189454516	-0.113472519
<i>Euparkeria_capensis</i>	-0.053127831	0.216166004	0.074526094	0.07307661
<i>Triopticus_primus</i>	1.065932304	-0.080304819	0.125268345	-0.013136809
<i>Revueltosaurus_callenderi</i>	0.055999841	0.211266442	-0.056929254	0.058114353
<i>Longosuchus_meadei</i>	0.195728315	0.228160307	-0.141555318	0.01598909
<i>Poposaurus_gracilis</i>	-0.493157015	-0.023778953	-0.068008617	-0.006507562
<i>Effigia_okeeffeae</i>	-0.035560466	-0.341424599	0.056995543	0.233562069
<i>Asilisaurus_kongwe</i>	-0.100470091	0.027594542	-0.035556141	0.162044721
<i>Silesaurus_opolensis</i>	-0.033169926	-0.105787583	-0.146830124	0.103218186
<i>Lesothosaurus_diagnosticus</i>	-0.151586122	-0.006103307	-0.252727482	0.009876337
<i>Sauropelta_edwardsorum</i>	0.163980262	0.15562907	-0.259851265	-0.222324374
<i>Gastonia_burgei</i>	0.163841038	0.086336877	-0.333963836	-0.050634973
<i>Stegoceras_validum</i>	0.373630773	-0.139300555	-0.040981561	0.055764513
<i>Eoraptor_lunensis</i>	-0.126851417	-0.074608667	-0.004847574	0.014954369
<i>Plateosaurus_engelhardti</i>	-0.033822301	-0.050586991	-0.017070941	-0.049296048
<i>Coelophysis_bauri</i>	-0.079496513	-0.233195111	0.077880386	-0.068109365
<i>Limusaurus_inextricabilis</i>	-0.107006188	-0.374622105	-0.059497618	0.021405606
<i>Allosaurus_fragilis</i>	-0.021326015	-0.162916886	0.030399415	-0.11693524
<i>Baryonyx_walkeri</i>	-0.054241238	-0.170745506	0.205484287	-0.131218942
<i>Spinosaurus_aegyptiacus</i>	-0.133364551	-0.108117028	0.140252442	-0.224955354
<i>Ornithomimus_edmontonicus</i>	-0.020095199	-0.331174005	-0.062013162	-0.009159358
<i>Protosuchus_richardsoni</i>	-0.087332568	0.161941319	-0.016967786	0.041182354
<i>Calsoyasuchus_valliceps</i>	-0.189449967	0.05566065	0.018199321	-0.066732485
<i>Pelagosaurus_typus</i>	-0.146910647	0.134358906	0.158061237	-0.020808404
<i>Gavialis_gangeticus</i>	-0.109903245	0.218539764	0.069573469	-0.079548015

Table S2: Convergence scores for the nMDS analysis using only cranial characters, related to Figure 3.

	NMDS1	NMDS2	NMDS3	NMDS4
<i>Protorosaurus_speneri</i>	-0.116541865	-0.004824474	0.113936652	0.180259497
<i>Malerisaurus_langstoni</i>	-0.103689354	0.267198217	0.227756432	0.084395486
<i>Prolacerta_broomi</i>	-0.204444356	-0.02664363	0.147547595	0.102751264
<i>Angistorhinus_alticephalus</i>	-0.176466046	0.320638447	-0.194672024	-0.091891338
<i>Euparkeria_capensis</i>	-0.205906978	0.008867174	0.066876911	0.081980166
<i>Triopticus_primus</i>	0.980978361	0.423050758	0.096696059	0.011579602
<i>Revueltosaurus_callenderi</i>	0.07615034	-0.127005177	-0.181057205	0.055394407
<i>Longosuchus_meadei</i>	0.188248588	-0.004999791	0.178729289	-0.172848965
<i>Poposaurus_gracilis</i>	-0.460086858	-0.138969404	-0.116357184	0.198812633
<i>Effigia_okeeffeae</i>	0.103190559	-0.165774359	0.284660812	-0.060751785
<i>Asilisaurus_kongwe</i>	-0.135300645	-0.177605823	0.093231376	-0.137228658
<i>Silesaurus_opolensis</i>	-0.061357035	-0.249809273	0.01246324	-0.174156872
<i>Lesothosaurus_diagnosticus</i>	0.008887579	-0.354823156	-0.20179907	-0.055570294
<i>Sauropelta_edwardsorum</i>	0.351895895	-0.183570251	-0.220335501	-0.114241643
<i>Gastonia_burgesi</i>	0.269597548	-0.322704544	-0.058046342	0.003073641
<i>Stegoceras_validum</i>	0.479446623	-0.062910409	-0.316809692	0.242421255
<i>Eoraptor_lunensis</i>	-0.123507713	-0.053454378	-0.002695595	0.130171423
<i>Plateosaurus_engelhardti</i>	0.016861315	-0.010844	-0.082584507	0.063138876
<i>Coelophysis_bauri</i>	-0.046358116	0.150191099	0.028241599	0.102192755
<i>Limusaurus_inextricabilis</i>	0.05541515	-0.287914072	0.268638343	0.042093283
<i>Allosaurus_fragilis</i>	-0.04654489	0.091986417	0.140716731	0.020665632
<i>Baryonyx_walkeri</i>	-0.061648678	0.381954208	-0.045496605	-0.033583636
<i>Spinosaurus_aegyptiacus</i>	-0.27036223	0.277244081	-0.113571342	0.1184214
<i>Ornithomimus_edmontonicus</i>	0.129335319	-0.16425068	0.186871	0.030061747
<i>Protosuchus_richardsoni</i>	-0.095415831	-0.03887496	-0.079243329	-0.085480083
<i>Calsoyasuchus_valliceps</i>	-0.176508781	0.036831147	-0.12852499	-0.176490629
<i>Pelagosaurus_typus</i>	-0.231348022	0.253114585	-0.000113636	-0.148243875
<i>Gavialis_gangeticus</i>	-0.144519876	0.16390225	-0.105059019	-0.216925291

Table S3: Convergence scores for the nMDS analysis using both cranial and postcranial characters, and additional Otis Chalk archosauromorph taxa, related to Figure 3.

	NMDS1	NMDS2	NMDS3	NMDS4
<i>Protorosaurus_speneri</i>	-0.065699747	0.143159598	0.053069377	-0.1238142
<i>Malerisaurus_langstoni</i>	0.022931006	0.152152103	0.140465916	-0.065826043
<i>Azendohsaurus_madagaskarensis</i>	0.017263378	0.127260545	0.044742597	-0.138016514
<i>Prolacerta_broomi</i>	-0.077180866	0.12054231	0.067744881	-0.119829844
<i>Trilophosaurus_buettneri</i>	-0.034718412	0.119605377	-0.035319799	-0.205884537
<i>Unnamed_Loricatan</i>	-0.330857294	-0.078429268	0.011850998	-0.076164911
<i>Doswellia_kaltenbachi</i>	-0.107104125	0.247591958	-0.000173849	0.033069902
<i>Angistorhinus_alticephalus</i>	-0.040101967	0.152179731	0.173679333	0.125784174
<i>Euparkeria_capensis</i>	-0.104072599	0.151493529	0.054041411	-0.057224176
<i>Triopticus_primus</i>	1.226428169	-0.020435484	0.085909039	-0.005453026
<i>Revueltosaurus_callenderi</i>	0.04878	0.169588748	-0.035131021	-0.029639604
<i>Longosuchus_meadei</i>	0.03314468	0.228725959	-0.170916326	0.031892309
<i>Poposaurus_gracilis</i>	-0.358600302	-0.12768435	-0.063331546	0.030835605
<i>Effigia_okeeffeae</i>	0.020612847	-0.306445289	-0.025461279	-0.195568198
<i>Asilisaurus_kongwe</i>	-0.081286791	-0.00196336	-0.031736829	-0.110942563
<i>Silesaurus_opolensis</i>	-0.001847113	-0.079149022	-0.124193384	-0.067987256
<i>Lesothosaurus_diagnosticus</i>	-0.101588473	-0.05076537	-0.213271474	0.053000215
<i>Sauropelta_edwardsorum</i>	0.124482371	0.145758793	-0.204157587	0.197837368
<i>Gastonia_burgesi</i>	0.114319372	0.111491513	-0.280121266	0.069031037
<i>Stegoceras_validum</i>	0.33885644	-0.071998401	-0.046134724	-0.037240258
<i>Eoraptor_lunensis</i>	-0.096743933	-0.085871153	0.011852215	-0.014312814
<i>Plateosaurus_engelhardti</i>	0.016369458	-0.051070229	0.010306897	0.034850015
<i>Coelophysis_bauri</i>	-0.016153456	-0.223404114	0.071440958	0.052307699
<i>Limusaurus_inextricabilis</i>	-0.025558039	-0.340613477	-0.084661259	0.012463286
<i>Allosaurus_fragilis</i>	-0.0257474	-0.168131666	0.035810061	0.065327885
<i>Baryonyx_walkeri</i>	-0.012434133	-0.164070822	0.141214062	0.156243804
<i>Spinosaurus_aegyptiacus</i>	-0.08414602	-0.14650794	0.208251946	0.078359443
<i>Ornithomimus_edmontonicus</i>	0.02626296	-0.296756201	-0.059860509	0.000434972
<i>Protosuchus_richardsoni</i>	-0.068531212	0.105101932	0.009631319	0.024485456
<i>Calsoyasuchus_valliceps</i>	-0.137133226	0.019479399	0.014128967	0.116371139
<i>Pelagosaurus_typus</i>	-0.124074063	0.085354947	0.149134536	0.06286886
<i>Gavialis_gangeticus</i>	-0.095871511	0.133809704	0.091196341	0.102740778

Supplemental Experimental Procedures

Institutional abbreviations used in this section

AMNH, American Museum of Natural History, New York, NY, USA; **BP**, Evolutionary Studies Institute, University of Witwatersrand, Johannesburg, South Africa; **BRLSI**, Bath Royal Literary and Scientific Institute; **BSP**, Bayerische Staatssammlung für Paläontologie und Historische Geologie, München, Germany; **CEUM**, Utah State University Eastern Prehistoric Museum, Price, UT, USA; **CMN**, Canadian Museum of Nature, Ottawa, ON, Canada; **ISI**, Indian Statistical Institute, Kolkata, India; **MCZ**, Museum of Comparative Zoology, Harvard University, Cambridge, MA, USA; **MSNM**, Museo di Storia Naturale di Milano, Italy; **NHMUK**, Natural History Museum of the United Kingdom, London, UK; **NHMW**, Naturhistorisches Museum Wien, Vienna, Austria; **NMT**, National Museum of Tanzania, Dar es Salaam, Tanzania; **PEFO**, Petrified Forest National Park, Petrified Forest, AZ, USA; **PVSJ**, Museo de Ciencias Naturales, San Juan, Argentina; **RTMP**, Royal Tyrrell Museum of Paleontology, Drumheller, Alberta, Canada; **SAM**, South African Museum, Cape Town, South Africa; **TMM**, Vertebrate Paleontology Laboratory, Jackson School of Geosciences, The University of Texas at Austin, Austin, TX, USA; **UALVP**, University of Alberta, Laboratory of Vertebrate Paleontology, Edmonton, Alberta, Canada; **UCMP**, University of California Museum of Paleontology, Berkeley, CA, USA; **UMMP**, University of Michigan Museum of Paleontology, Ann Arbor, MI, USA; **UMZC**, Museum of Zoology, Cambridge University, Cambridge, England; **UUVP**, University of Utah Vertebrate Paleontology Collection, Salt Lake City, Utah (now UMNH VP); **YPM**, Yale Peabody Museum of Natural History, New Haven, CT, USA; **ZPAL**, Institute of Paleobiology of the Polish Academy of Sciences in Warsaw, Poland.

Extended morphological description of *Triopticus primus*

Structure of cranial bosses

The median frontal boss is most similar to the ‘dome’ of pachycephalosaurs (Fig. 2G). When the braincase is positioned in ‘alert posture’ with the lateral semicircular canal of the inner ear horizontal [S11, S12], the rounded apex of the frontal boss faces dorsally and its anterior surface faces mostly forward, sloping ventrally as it approaches the missing facial region. A pair of postorbital bosses reside posterolateral to the frontal boss and posterodorsal to the orbits. These bosses are separated by furrows from the squamosal-parietal bosses, which occupy the posterolateral corners of the skull and meet each other at the back of the skull. As in pachycephalosaurs (and other marginocephalian dinosaurs), the paired squamosal-parietal bosses overhang the occiput (Fig. 2). The internal structure of the bosses was studied in the CT scan data (see horizontal slice in Fig. 2A). The regions corresponding to the paired bosses are generally distinct from the region of the frontal boss. The bosses are not entirely discrete internally, but there are discernable patterns of differing density associated with the bosses. Moreover, there are some ‘seams’ of high-density material (appearing whitish in Fig. 2A) that may mark rough boundaries between the bosses. A valid question to ask is whether these bosses represent fusion of the normal skull roofing bones with discrete ossification centers within the dermis (i.e. osteoderms) or whether they represent outgrowths of the roofing bones themselves. Vickaryous et al. [S13] addressed this same question for ankylosaurian dinosaurs and found evidence for both phenomena (i.e. both fusion of osteoderms and bony outgrowth) in ankylosaurs, but for *Triopticus*, in the absence of histological analysis and additional (preferably ontogenetically younger) specimens, the question must remain open.

Cranial endocast and endosseous labyrinth

The hypermineralization that characterizes the entire holotype braincase of *Triopticus* has resulted in a very complete cranial (brain) endocast, meaning that areas that typically are open in the skulls of most archosauriforms, such as those covering the anterior and ventral portions of the telencephalon (cerebrum and olfactory system) are completely covered by bone in *Triopticus*. As a result, much of the endocast can be segmented from the CT scan data, although some details are obscured by fractures. Also, it should be noted that interpretation of the CT data is made challenging by the fact that the fossilized bone and rock matrix are similar enough in density that a number of details, such as some small canals and the precise

shapes of some contours, are not fully resolvable. Nevertheless, the major features of the brain endocast are tolerably clear. Comparisons are made here to published accounts of early-diverging archosauriform endocasts (e.g. [S14-19]), as well as unpublished analyses of CT scan data of *Chanaresuchus bonapartei* (MCZ 4037), *Gracilisuchus stipanicorum* (MCZ 4117), *Parasuchus hislopi* (ISI R44), *Postosuchus* sp. cf. *P. kirkpatricki* (UMMP 7473), *Desmotosuchus spurensis* (UCMP 27408, UCMP 27410), and *Herrerasaurus ischigualastensis* (MCZ 7063). Comparisons also are made to the endocasts of pachycephalosaurs [S19], principally based on original work on *Stegoceras validum* (UALVP 2), the endocast of which was illustrated as incidental parts of other figures by Bourke et al. [S20].

The brain endocast in *Triopticus* (Fig. 2, S1) generally is symmetrical and not markedly deformed, other than some missing bone in the midbrain region caused by fracture of the specimen. The general orientation of the endocast is elongate with very little of the midbrain flexure observed in some other early-diverging archosauriforms, such as phytosaurs ([S14, S17]; ISI R44) and aetosaurs ([S15]; UCMP 27408, UCMP 27410). Endocasts are direct reflections of the conformation of the dural envelope rather than of the brain itself, and archosaurs differ in the extent to which their endocasts faithfully reflect the surface anatomy of the underlying brain [S12].

In *Triopticus*, the telencephalic region of the endocast appears to be relatively ‘brain-like’ in comparison to other early-diverging archosauriforms, in that the two cerebral hemispheres are fairly distinct and separated by a median interhemispheric sulcus, the region of the olfactory tracts is narrow, and the olfactory bulbs are very well demarcated. This morphology stands in contrast to that of many other early-diverging archosaurs in which these brain regions are not very well distinguished from each other. Actually, the telencephalon of the pachycephalosaur *Stegoceras* is very similar to that of *Triopticus* (Fig. S1K–L), and it is tempting to suggest that this similarity further reflects the convergence discussed in the main text. A hypothesis that merits further testing is that a ‘tighter’ endocast (i.e. less non-neural space within the endocranium, producing a more brain-like endocast) might be a functional adaptation for use of the head in agonistic behaviors in that a decreased distance between brain and braincase would decrease the inertial effects causing concussive damage to the neural tissue. Another explanation is that this more brain-like telencephalic endocast may simply reflect the hypermineralization of the braincase that occurred in both *Triopticus* and pachycephalosaurs. These hypotheses are not mutually exclusive.

The midbrain region of *Triopticus* shows no direct indication of the morphology of the optic lobes, which reflects the fact that the dural envelope in this region did not closely follow the contours of the brain, which is typical of many archosaurs. It seems likely that, as in most non-coelurosaurian archosaurs [S12, S21-23] other than pterosaurs [S11], the optic lobes were in the plesiomorphic position of contacting each other in the midline between the cerebrum and cerebellum. The optic nerve trunks (CN II) are relatively large, which, coupled with the large size of the orbits, suggests the presence of large eyeballs and the importance of vision for *Triopticus*. The details of the hindbrain region were again largely obscured by the overlying dura, although one key component of the cerebellum, namely its floccular lobe, is well preserved, especially on the left side.

The cerebellar flocculus is very large in *Triopticus*, and, although quantitative comparison is not feasible at this time (because of the variability in completeness of specimens), the flocculus clearly is relatively much larger than in other Triassic archosauriforms (Fig. S1). The presence and size of the flocculus is variable among these early taxa. There is no indication of any flocculus at all in the early-diverging archosauriform *Chanaresuchus bonapartei* (MCZ 4037; Fig. S1P), although the braincase is incomplete, and, in other related taxa such as *Erythrosuchus*, *Euparkeria*, and *Osmolskina*, the floccular (auricular) fossa is described as ‘shallow’ at best [S24-26]. Likewise, among early-diverging archosaur clades, many taxa either lack a flocculus altogether, such as the aetosaur *Desmotosuchus spurensis* (UCMP 27408, UCMP 27410; Fig. S1S), or it is extremely small, such as in the early-diverging phytosaur *Parasuchus hislopi* (ISI R44; Fig. S1Q). Others have a relatively small flocculus, such as the early-diverging suchian *Gracilisuchus stipanicorum* (MCZ 4117; Fig. S1R), the rauisuchid *Postosuchus* sp. cf. *P. kirkpatricki* (UMMP 7473; Fig. S1T), and the early-diverging theropod *Herrerasaurus ischigualastensis* (MCZ 7063; Fig. S1U). Given that the flocculus in extant vertebrates has been shown to be involved in coordinating eye, head, and neck movements to stabilize gaze (i.e. the vestibulo-ocular and vestibulocollic reflexes; [S11, S12, S27]), the large size of the cerebellar flocculus in *Triopticus*, coupled with its elongate semicircular canals (which sense turning movements of the head), large optic nerves, and large orbits all suggest that *Triopticus* was a very visually oriented animal that placed a high premium on visual tracking movements. It also may be noted that the flocculus of the pachycephalosaur *Stegoceras* (Fig. S1V) is

extremely small, suggesting that the strong convergence seen in the structure of the cranial dome and bosses did not extend to the sensorineural apparatus mediating the vestibular reflexes.

Other than the flocculus, little else about the cerebellum of *Triopticus* can be judged based on the endocast. Likewise, other elements of the endocast that can be extracted (Fig. 2, S1), such as the brainstem, trigeminal nerve (right side only), and hypoglossal nerves (two trunks on each side), are all basically unremarkable and similar enough to a wide variety of archosaurs.

The midline dorsal pit in the braincase of *Triopticus* is essentially between the frontal and parietal bones, which places it in the position of the pineal foramen of many extinct reptiles [S28]. Consequently we explored the possibility that this feature could be a hypertrophied pineal gland (epithalamic epiphysis). The pineal-parapineal complex is highly variable in vertebrates [S29], as is the status of an aperture in the skull. Among extant reptiles, only crocodylians lack the pineal complex [S30]. Birds generally have a well-developed pineal that extends dorsally between the cerebrum and cerebellum to attaches to the dura, but never creates an aperture [S31]. Witmer and Ridgely ([S23]; see also [S12, S32]) identified a “pineal peak” in a diversity of dinosaurs wherein the endocast has a median dural extension that forms a peak directly behind the cerebral region although does not form an aperture in the skull. Thus, it remains possible if not likely that *Triopticus* indeed had a pineal, regardless of whether it made an opening in the skull roof. A meticulous examination of the CT scan data failed to find any unambiguous connection between the endocranial cavity and the dorsal pit. In almost all CT slices (e.g. Fig. 2), there was demonstrable bone separating the two spaces. The only potential connections visible were clearly cracks in the fossil. The scan data are not sufficiently clear to categorically rule out a connection, but it seems unlikely. Moreover, the endocast even lacks a dural peak in the relevant area. Thus, the absence of a clear connection between the dorsal pit and the endocranium, coupled with the evidence noted previously (e.g. dermal surface ornamentation within the pit), makes it likely that the dorsal pit has nothing to do with the pineal gland.

The endosseous labyrinth of the inner ear of *Triopticus* is virtually complete on the left side and partially preserved on the right side (Fig. S1A–F). As with the flocculus, the labyrinth is strongly divergent from that of most other Triassic archosauriforms. The entire structure is relatively very large, and all three semicircular canals are elongate. Again, quantitative comparison presently is problematic for a number of reasons, such as incompleteness of the labyrinth in many relevant fossils, but the qualitative differences are readily apparent (Fig. S1). The anterior semicircular canal is by far the longest and has a well-preserved and swollen ampulla. Elongate anterior canals have sometimes been associated with bipedality (e.g. [S33]), and thus may shed some light on the habits of *Triopticus*, although the causal nature of this association is unclear given that the canals are neurologically associated with visual parameters such as stabilizing gaze [S34]. The lateral (horizontal) canal also is relatively very long and also has a well-marked ampulla. The function in this case may relate to the importance of lateral visual scanning movements of the eyes and head [S23]. The position of the lateral semicircular canal has sometimes been associated with the head posture that animals adopt when they are being particularly wary, such that ‘alert postures’ of extant animals tend to average around 0° corresponding roughly to Earth horizontal [S11, S12, S34]. When the cranium of *Triopticus* is placed in its ‘alert posture’ with the lateral canal horizontal, the apex of the frontal boss is directed dorsally and the main portion of the frontal boss faces anteriorly (Fig. 2). The cochlear duct in *Triopticus* is moderately long (Fig. S1A–F) and comparable to the length of the hearing organ in most other Triassic archosauriforms, where known (Fig. S1). The endosseous labyrinth of *Triopticus* is not particularly similar to that of pachycephalosaurs such as *Stegoceras* (Fig. S1K–L), and the overall conformation is actually much more similar to some theropods [S23, S32], such as *Herrerasaurus* (Fig. S1U).

Brief overview of Otis Chalk faunal assemblage and age

Late Triassic tetrapods have been described from the Otis Chalk localities since the 1920s [S35–42], and a major assessment of the faunal assemblage was presented by Elder [S43, S44] in order to document taphonomic processes and interpret the paleoecology. Approximately 11,000 specimens were collected by the WPA (J. C. Sagebiel pers. comm. 2012) through quarrying operations at four main localities (Quarry 1: TMM 31025; Quarry 2: TMM 31099; Quarry 3: TMM 31100; Quarry 3A: TMM 31185) and through surface collection of several other general localities (Site 3 General: TMM 31098; Site 7 General: TMM 41936) in Howard County. The precise stratigraphic relationships among the individual localities are unclear, though they are all within the Colorado City Member of the Dockum Group [S43]. In general, the Otis Chalk localities produced assemblages that are taxonomically multidominant (*sensu* [S45]) though

some individual localities were interpreted as multitaxic and monodominant (i.e. TMM 31025 is known colloquially as the ‘*Trilophosaurus* Quarry’; [S43]). A full redescription of the assemblage is in preparation ([S46]; MRS unpublished data).

The Otischalkian type assemblage had been hypothesized to be Carnian (Tuvalian) in age based on the presence of the phytosaur “*Paleorhinus*” (= *Parasuchus*) and the aetosaur *Longosuchus meadei* [S47, S48]; no numerical dates currently exist for the locality. However, because of documented problems associated with the use of “*Paleorhinus*” for biochronologic correlations [S46, S49-51], the correlation of the Otis Chalk assemblage with the Carnian is unsupported. Several taxa from the Otischalkian assemblage (e.g. *Colognathus obscurus*, *Trilophosaurus buettneri*, *Doswellia kaltenbachi*, *Dromomeron gregorii*) are found in the Blue Mesa Member of the Chinle Formation of Arizona, which represents the type fauna of the Adamanian biozone [S48, S52] and has been dated (maximum depositional ages) to the early Norian using high precision U-Pb analysis of detrital zircons (220.124±0.068 Ma for the Blue Forest area of Petrified Forest National Park; [S53]; and 219.39±0.16 Ma for the *Placerias* Quarry; [S54]).

Better taxa for biochronologic correlation may be *Lucasuchus hunti* and *Coahomasuchus kahlerorum*, which otherwise only occur in the Pekin Formation of North Carolina, which, based on magnetic polarity data, is older than 226 Ma [S55-58]. The magnetostratigraphy of the Poor Farm Member of the Falling Creek Formation (Newark Supergroup) correlates with chrons E7n and E6r of the Newark Supergroup astrochronology and geomagnetic polarity timescale (Newark APTS; [S59, S60]). This dates the occurrence of the holotype specimen of *Doswellia kaltenbachi* [S61] to approximately 229 Ma. Thus, based on the presence of *Doswellia kaltenbachi*, *Lucasuchus hunti*, and *Coahomasuchus kahlerorum*, the Otis Chalk quarries may date between 229 to 226 Ma, which is latest Carnian-earliest Norian under the “long-Rhaetian” option in recent discussions of the Triassic Timescale [S62-64].

Phylogenetic analysis of *Triopticus primus*

Taxon and character sampling explanation

We included *Triopticus primus* in the phylogenetic matrix of Nesbitt et al. ([S7]; expanded from [S65]), which focused on resolving the relationships among early archosauromorph reptiles. We chose this dataset because the following combination of character states in *Triopticus* are also present in some archosauromorph taxa: presence of a single occipital condyle; ossified laterosphenoid; presence of a metotic strut of the otoccipital; presence of upper and lower temporal fenestrae; presence of an antorbital fenestra and fossa formed by the lacrimal. Because of the incomplete preservation of the holotype of *T. primus*, a broad sampling among archosauromorph reptiles was necessary. We used a minimum of three terminal taxa to code for diverse archosauromorph clades (e.g. Rhynchosauria, Archosauria; [S66]). Following Nesbitt et al. [S7], we excluded *Macrocnemus fuyuanensis* (included by [S65]), but included *Pamelaria dolichotrachela*, *Azendohsaurus laaroussii*, *Azendohsaurus madagaskarensis*, *Spinosuchus caseanus* (based on the work of [S67]), “*Chasmatosaurus*” *yuani*, *Coelophysis bauri*, and *Plateosaurus engelhardti*. We additionally included *Chanaresuchus bonapartei* as an additional non-archosaurian archosauriform. We only included *Proterosuchus* rather than also including *Proterosuchus alexanderi* as was done by Nesbitt et al. [S7]. This sampling resulted in 30 ingroup taxa, including *Triopticus primus*, and one outgroup (*Petrolacosaurus kansensis*). Character states for each terminal taxon follow Nesbitt et al. [S7], based on firsthand observations, published morphological descriptions, and photos taken by Pritchard et al. [S65] and Nesbitt et al. [S7]. Character states for *Triopticus primus* are based on first-hand observations of the specimen by the authors, supplemented with data from computed tomographic analysis. Character sampling includes the dataset of Pritchard et al. [S65] with the modifications and additions of Nesbitt et al. [S7], resulting in a total of 247 characters. Characters 2, 5, 10, 11, 20, 32, 52, 72, 204, and 212 were ordered because these multistate characters represent potential nested sets of character states.

Tree search strategy

We used the Tree Analysis using New Technology software package (TNT) version 1.1 [S68] following the analyses of Pritchard et al. [S65] and Nesbitt et al. [S7]. We used a traditional search (1000 replicates of Wagner trees, using random addition sequences) followed by tree bisection and reconnection (TBR) branch swapping, holding 10 trees per TBR replicate. Zero-length branches were collapsed if they lacked support under any of the most parsimonious reconstructions.

Results of the phylogenetic analysis

We recovered five Most Parsimonious Trees (MPTs) with tree length of 622. In the strict consensus *Triopticus primus* is in a polytomy with *Proterosuchus*, “*Chasmotosaurus*” *yuani*, *Erythrosuchus africanus*, *Chanaresuchus bonapartei*, *Euparkeria capensis*, and Archosauria within Archosauriformes (Fig. 1A). The topology of the strict consensus does not change regardless of *Triopticus* being coded as ‘present’ or ‘uncertain’ for the presence of a pineal foramen. We found *Triopticus primus* as an archosauriform in every MPT and more closely related to Archosauria than to any other diapsid crown group. *Triopticus primus* is supported as an archosauriform based on the presence of an antorbital fenestra (13-1) and an ossified laterosphenoid (72-1).

List of taxa included in phylogenetic analysis of *Triopticus primus*, including representative specimens and/or literature used for character coding.

Taxon	Sources
<i>Amotosaurus rotfeldensis</i>	[S69]
<i>Azendohsaurus madagaskarensis</i>	[S7]
<i>Azendohsaurus laaroussii</i>	MNHN-ALM 424-5, MNHN-ALM 424-4, MNHN-ALM 351, MNHN-ALM 365-20, MNHN-ALM 353, MNHN-ALM 365-17, MNHN-ALM 365-18, MNHN-ALM 355-3, MNHN-ALM 365-21, MNHN-ALM 365-16; [S7, S70]
<i>Batrachotomus kupferzellensis</i>	[S71-73]
“ <i>Chasmotosaurus</i> ” <i>yuani</i>	Cast of holotype IVPP V36315, V2719, V2720, V4067; [S74, S75]
<i>Chanaresuchus bonapartei</i>	[S5]
<i>Coelophysis bauri</i>	[S5]
<i>Erythrosuchus africanus</i>	NHMUK R 3592, BP/1/5207; [S76]
<i>Euparkeria capensis</i>	SAM specimens; [S77]
<i>Gephyrosaurus bridensis</i>	[S78, S79]
<i>Langobardisaurus pandolfii</i>	MCSNB 2883, 4860; MFSN 1921; [S80]
<i>Macrocnemus bassanii</i>	MCSN BES SC 111, V 457; [S81]
<i>Mesosuchus browni</i>	SAM specimens; [S82]
<i>Pamelaria dolichotrachela</i>	ISIR 317, ISIR 318-333
<i>Petrolacosaurus kansensis</i>	[S83]
<i>Plateosaurus engelhardti</i>	[S5]
<i>Prolacerta broomi</i>	BP/1/2675, 2676, 5375; [S84]
<i>Proterosuchus</i>	Following [S7]; NMQR 1484; SAM-PK-K140; [S85-87]
<i>Protorosaurus speneri</i>	USNM 442453, YPM 2437; [S88]
<i>Rhynchosaurus articeps</i>	NHMUK R 1235, 1236; [S89]
<i>Shinisaurus crocodilurus</i>	[S90-92]
<i>Spinosuchus caseanus</i>	NMMNH P-57852 to P-57865; [S7, S67]
<i>Tanystropheus longobardicus</i>	MCSN BES SC 61, SC 265, BES SC 1018, V 3663, V 3730; [S93, S94]
<i>Tanytrachelos ahynis</i>	AMNH FARB 7206; YPM 7482, 8600; VMNH #2826, 3423, 120015, 120016
<i>Teyumbaita sulcognathus</i>	[S95, S96]
<i>Teraterpeton hrynewichorum</i>	[S97]
<i>Trilophosaurus buettneri</i>	Hundreds of specimens from TMM, largely TMM 31025-140

<i>Trilophosaurus jacobsi</i>	Hundreds of specimens from NMMNH; [S98]
<i>Triopticus primus</i>	TMM 31100-1330; this study
<i>Uromastyx</i> sp.	Complete skeleton in Stony Brook University comparative anatomy collection; [S99]
<i>Youngina capensis</i>	BP/1/375, BP/1/2871; [S100-102]

Character-taxon matrix for phylogenetic analysis of *Triopticus primus*

[0,1] = A
 [0,2] = B
 [1,2] = C
 - = I

Petrolacosaurus kansensis

0000II0000000001000000010110000201011001000000010101000000000010110000?
 0???10000000011I000000000000011I00000010?100000000100II0000I00010?0001
 00011?0100110001100?0100000I0I110000010?I100000000000I0I0?00100000?00I0
 000100000000000I0I000000?0?0I01000

Youngina capensis

0000II00001000010100000101010002000100110000000111110000010000010100100
 01101000????0?00010100000000010I??00?000I01010000??000II000101001???111
 000?10110111?0001??0110?010I0?111?01?0???10000?000000I0I0??0100000?00I0
 0001?0000000000I0000?010?000I??0?1

Gephyrosaurus bridensis

0000II00002I01000110100001000001000000I11010000110I100????0000?10100?00
 0?????01?0??0?0101000001I000010I00?0?000I00000?000?000II?111011110???111
 000010?11011?????????1110011I0111?000000?01100?01?????110??00000000?10I0
 111??001?000000I0I?1?????0?00100?0

Shinisaurus crocodilurus

0000II00101I011001101000III000001I0101II1110101100I01I10010001110100110
 000101011110010101010001I000012100001000I1000000000000II1100I1011111111
 000110010011100110101100010I1011100001000011010?1?001010000?1?0100100I0
 00?0011010000?0I0I10001010000100?0

Uromastyx sp.

0000II00102I01100?101010I0??00101I0001II1111I0IIIII01I11010I01010100100
 01100101101?01010100001III0I002100000000I1000000000000II1110I1011011111
 000110110011100110101110?11I101111000010001100001I1111100000100?00?0?I0
 10010?000?000?0I0I0000001000000000

Protorosaurus speneri

0000II0000100000001101I?01100001000100I11010?????????????10??00010?????????
 ??????001?000?0001000000?00?010I1110??1110000000??000II0000I?0010??1?1
 10001?01010001010000000?????1?111?011?????10000000001?1000?0100?0??00I?
 000100000000000?0I00?0000000000?0?

Langobardisaurus pandolfii

100????00????0????????????????00???
 ??????0?????0???11000200?00?01211111?1111001?101?????1???1?011110?000111
 10?????010100I11??0?010??11111??1111110??0100?1?001??10111?????????????
 0?0?0??0000?0?0??1??00?000????0??

Euparkeria capensis

00011100001010010001?1I111110002011000001010?00110?100??1?1?11110?11?11
210?010011011?00011100001010011I010000100?00?000??2??1100000I??0?0??11?
?00??0??1?0I11?????0001?1111??1?0I011100001100I111110000101110101010
1011011000111011011000100I000??01?

Batrachotomus kupferzellensis

0001011010101000000111I0I1100002011000001011I0III0I1001011101011?001?10
20?1???00?100100001110000101I011I011000110A001001112101001000I??0100011?
??0010010100010?????000101111011001I01?1001011?0I??110??0112110111020
1011?110?01110?1121?0?1?0I000?1011

Coelophysys bauri

0101I10000101000000111I0I1100102011000001?011?11I0I100100?1001110?0111?
20?10100??00110001110000101I011I1110001110001001111100II1100I10010?01II
II011000I1000100011I0001011110011000I01110A10III0I11100II00112010111020
001?11101111111I1I1000001I000010??

Plateosaurus engelhardti

0001I10000101000000111I0I11001020110000010011?11I0I?00100?1001110001110
C0010100?100110001100000100I011I1110001100001001111100II1100I1001??01?I
II011000I1000100011I0001011110011?00I01110010III0I11100II00112010111020
001001111111111I1I1000011I00000011

Triopticus primus

?????????????11??0?10?????????????0?1?????????1?????????10111?11110??2???
2?01???
??00?????
???

Convergence analysis

Specifying the details of convergence between and among taxa is difficult despite the ability to agree that those taxa follow a general gestalt. General bauplan similarities between Triassic archosauromorphs and post-Triassic archosaurs, especially dinosaurs, have long been recognized (e.g. [S103-108]). In some instances, those similarities were found on incomplete or isolated specimens, or were treated as ‘key characters’ and used as evidence of the presence of clades in regions or times previously not known for those taxa. However, incorporation of those taxa into phylogenetic frameworks subsequently allowed those character states to be put into phylogenetically-informative contexts. That apomorphy-based approach thus revealed homoplasy and convergence throughout Archosauromorpha (e.g. [S5, S109, S110]).

In order to provide a quantitative measure of morphological similarity between Triassic archosauromorphs and post-Triassic archosaurs, we developed a new approach to analyze morphological convergence. Previous quantifications of morphospace occupation focused on competition between dinosaurs and other archosauromorphs, with the emphasis on the overall morphospace occupation and rates of morphological character change as related to potential competition among those major groups, and later ‘success’ of the post-Triassic archosaurs, rather than on inferences of convergence (e.g. [S66, S103, S111]). We instead focus on examining the overlap in morphospace itself. Convergence in morphospace can be expressed in two main patterns [S112]: 1) the convergent species occupy the same area of morphospace; and 2) convergent taxa deviate from their relatives toward the same area of morphospace but do not actually occupy the same area. We would expect to see the second pattern expressed more often among such a broad range of taxa because of the influence of phylogeny, as well as function, on the subsequently expressed morphology.

We focused our choice of Triassic taxa on those found in the Otis Chalk faunal assemblage because that assemblage preserves a diverse group of archosauromorph taxa with a wide range of disparate cranial morphologies, dental modifications, and overall body plans. Additionally, the Otis Chalk assemblage is the basis for the Otischalkian biozone ([S48]; sensu [S52]), the earliest terrestrial

biochronologic division of the Late Triassic, and may represent one of the oldest and best-documented Late Triassic terrestrial assemblages in North America (e.g. [S35–44, S46]). The Otis Chalk assemblage is well known for the multiple specimens of the aberrant archosauromorph *Trilophosaurus* that were collected by the Works Progress Administration from 1939 to 1940 [S37], but it also produced specimens of the phytosaurs *Parasuchus* and *Angistorhinus*, multiple aetosaurs (*Longosuchus*, *Lucasuchus*, *Coahomasuchus*), and the loricatan *Poposaurus langstoni* [S43, S46, S57, S113]. We did not include all members of the Otis Chalk assemblage here because we focused on the archosauromorphs that had recognized similarities with later (=post-Triassic) archosauromorphs. For example, we did not include *Trilophosaurus* in our main analysis (but see below) because there is no known archosauromorph from later in the Mesozoic or Cenozoic that is convergent on the morphology of *Trilophosaurus*; however, *Angistorhinus* was included to acknowledge the often-cited similarities between phytosaurs and extant crocodylians (e.g. [S114, S115]).

We then chose at least one post-Triassic archosaur that has morphological similarity to an Otis Chalk taxon, thus creating sets of similar Triassic and post-Triassic taxa. Our choice of post-Triassic taxa depended on several criteria: we selected taxa that are known from fairly complete skeletons, that are published in peer-reviewed literature, have well-supported relationships, and have the most characters in common with a Triassic archosauromorph. Clearly not all convergent characters appeared simultaneously and would have appeared in a mosaic pattern through time, so we looked for archosaurs that had the highest accumulation of convergent characters with a Triassic archosauromorph. In several cases, skeletal completeness (e.g. has a cranium and postcranium, known from more than one individual, is three-dimensionally prepared) outweighed a more basal position within the taxon's respective clade. This sampling resulted in a total of 28 archosauromorph taxa (1 Late Permian, 14 Triassic, and 13 post-Triassic) in our analysis (see below); *Protorosaurus speneri* was used as the outgroup taxon with respect to plesiomorphic or ancestral morphologies and age. Documenting that the convergent morphologies appeared subsequent to the end of the known record of the Triassic taxon is important to show that those convergent morphologies later appeared independently of the Triassic lineages. Using published and well-supported phylogenetic relationships of our Triassic and post-Triassic taxa we created a time-calibrated, grafted tree (Fig. S2) with 'morphological bracketing' to document the timing of character state appearance.

We identified 81 morphological characters associated with specialized ecomorphologies, and often the most recognized morphological features, of the skeletons of our chosen taxa that were cited as convergently evolved between Triassic archosauromorphs and post-Triassic archosaurs (e.g. [S104, S107, S114]). Our character list comprises a mix of previously published phylogenetic characters as well as some newly developed characters that sample features throughout the skeleton. However, an important aspect of our analysis is that this is a separate set of characters than that used for determining the phylogenetic position of *Triopticus*. Therefore, the phylogenetic relationships of *Triopticus* were determined through an independent analysis (see above), and the characters in our convergence analysis do not necessarily imply homology between taxa. The complete matrix for the convergence analysis is available online through MorphoBank [S116] at <http://morphobank.org> under Project 1187.

We analyzed our matrix of 28 taxa and 81 morphological characters using non-metric multidimensional scaling (nMDS). This allowed ordination of our pooled multivariate data into two and three dimensions for ease of interpretation. We used nMDS rather than principal component analysis (PCA) or principal coordinate analysis (PCO) because nMDS is better able to incorporate missing data among discrete characters by maintaining ranked differences rather than absolute differences [S117, S118]. We utilized the Claddis [S119] and vegan [S120] packages in the R software environment [S121] to run the nMDS analysis, which allowed for the incorporation of more dimensionality than does the program PAST [S117]. We used Claddis, which is able to incorporate missing data and polymorphic characters, to import the character matrix as a Nexus file and convert the matrix of discrete, categorical data to a distance matrix. Claddis rescales distances using a combination of the Generalized Euclidean Distance [S122], the Gower dissimilarity [S123], and a third method based on the maximum possible observable distance [S119]. We imported our matrix using ReadMorphNexus, computed distances using morph.dist.matrix, and removed incalculable values using TrimMorphDistMatrix. We then ran the nMDS analysis in vegan using the metaMDS command, with four dimensions and a maximum of 1000 random starts in search of a stable solution. Two convergent solutions were reached after four tries.

List of Otis Chalk assemblage taxa included in convergence analyses, including representative specimens and literature for character coding

Taxon		Voucher Specimen(s)	Element	Reference
Archosauromorpha				
	<i>Trilophosaurus buetneri</i>	TMM 31025-140	Partial skeleton	[S37]
	<i>Malerisaurus langstoni</i>	TMM 31099-11	Partial skeleton (holotype)	[S36]
	Tanystropheid	TMM 31100-1196	Presacral and caudal vertebrae	New occurrence
Archosauriformes				
	<i>Triopticus primus</i>	TMM 31100-1030	Partial skull (holotype)	This study
	<i>Doswellia kaltenbachi</i>	TMM 31025-152	Partial skeleton	[S113]
Phytosauria				
	<i>Parasuchus bransoni</i>	TMM 31100-101	Skull	[S113]
	<i>Angistorhinus alticephalus</i>	OMNH 733; TMM 31100-1332	Partial skull and associated skeleton (holotype); skull and articulated partial skeleton	[S113]
	<i>Brachysuchus megalodon</i>	UMMP 10336	Skull (holotype)	[S35]
Aetosauria				
	<i>Coahomasuchus kahleorum</i>	NMMNH P-18496	Articulated partial skeleton (holotype)	[S124]
	<i>Longosuchus meadei</i>	TMM 31185-98	Skull (lectotype)	[S125]
	<i>Lucasuchus hunti</i>	TMM 31100-257	Paramedian osteoderms (holotype)	[S113]
Paracrocodylomorpha				
	Unnamed new taxon	TMM 31098-46	Maxilla	[S46]
	<i>Poposaurus gracilis</i>	UMMP 11748	Right ilium	New occurrence
	<i>Poposaurus langstoni</i>	TMM 31025-12	Right ilium (holotype)	[S113]
	Shuvosauridae	TMM 31100-1211	Right ilium	[S46]
Crocodylomorpha				
	Unnamed taxon	TMM 31100-1494	Right ilium	[S46]
Dinosauromorpha				
	<i>Dromomeron gregorii</i>	TMM 31100-1306	Right femur (holotype)	[S126]
	Silesauridae	TMM 31100-185	Left femur	[S127]
	Theropoda	TMM 31100-545	Right femur	[S46]
	<i>Chindesaurus bryansmalli</i>	TMM 31100-523	Proximal portion, left femur	[S113]
	<i>Lepidus praecisio</i>	TMM 41936-1.3	Articulated ankle region	[S6]

Taxa used in convergence analysis

Protorosaurus speneri, sensu [S88].
Age range: Tatarian, Late Permian [S128].
Specimen(s) examined: NHMW 1943I4 (lectotype specimen). See [S88] for a complete list of specimens.
Explanation for selection: *Protorosaurus speneri* is included here because it represents the most basal taxon in Archosauromorpha [S82] and has a similar body plan as other early archosauromorphs.

Prolacerta broomi, sensu [S84].

Age range: Induan, Early Triassic [S129].

Specimen(s) examined: UMZC 2003.40, partial skull and mandible; BP/1/471, complete skull; BP/1/2675, postcranial skeleton and nearly complete skull; BP/1/2676, nearly complete skeleton; UCMP 37151, skull; AMNH 9502, postcranial skeleton.

Explanation for selection: *Prolacerta broomi* represents a well-preserved non-archosaurian archosauromorph that is used in phylogenetic analyses of the Archosauromorpha (e.g. [S130]). Furthermore *Prolacerta broomi* possesses elongate cervical vertebrae [S102] similar to those in many other archosauromorphs included in this analysis. In Upper Triassic deposits the elongate vertebrae of archosauromorphs have been commonly misidentified as belonging to theropod dinosaurs (e.g. [S131]), and therefore we test this convergence.

Euparkeria capensis, sensu [S77].

Age range: Anisian, Early Triassic [S129].

Specimen(s) examined: SAM 5867, partial skeleton and skull – holotype specimen.

Explanation for selection: *Euparkeria capensis* is a well-known non-archosaurian archosauriform based on well-preserved material and is often incorporated as the outgroup taxon in phylogenetic analyses of Archosauria (e.g. [S132]). Its bauplan likely represents the plesiomorphic body type for Archosauria.

Asilisaurus kongwe, sensu [S127].

Age range: Middle Triassic [S129]; Silesauridae has an age range of late Anisian to late Norian [S127].

Specimen(s) examined: NMT RB 9, holotype specimen; NMT RB159, skeleton, dozens of isolated bones [S127].

Explanation for selection: Silesaurids are purportedly quadrupedal dinosauriforms with a dentition consisting of leaf-shaped teeth and a beak-like lower jaw similar to what is found in ornithischian dinosaurs [S133]. *Asilisaurus* bears a number of synapomorphies with silesaurids, but retains many of the plesiomorphies of dinosauriforms and ornithodirans [S127]. Furthermore, most of the anatomy of the taxon is represented among the dozens of specimens.

Silesaurus opolensis, sensu [S133].

Age range: late Carnian, Late Triassic [S133]; Silesauridae has an age range of late Anisian to late Norian [S127].

Specimen(s) examined: ZPAL Ab III/361/26, right maxilla (part of holotype); ZPAL Ab III/437/1, left dentary.

Explanation for selection: Silesaurids possess several cranial characters that may be convergent with ornithischian dinosaurs including leaf-shaped teeth and a beaked dentary [S127, S133]. *Silesaurus* is the best-preserved silesaurid with nearly the complete skeleton known from numerous specimens [S133, S134]. We use *Silesaurus* as a surrogate taxon for the unnamed Otis Chalk silesaurid (e.g. TMM 31100-185, left femur) because *Silesaurus* is known by multiple specimens that inform on the anatomy of the entire skeleton and the Otis Chalk taxon shares multiple synapomorphies of Silesauridae with *Silesaurus* [S46, S127, S133].

Effigia okeeffeae, sensu [S107].

Age range: middle Norian, Late Triassic [S135]; Shuvosauridae has an age range of Anisian to Rhaetian [S5].

Specimen(s) examined: AMNH FR 30587 – partial skeleton including skull (holotype specimen).

Explanation for selection: Shuvosaurids are bipedal, edentulous pseudosuchians that share convergences with theropod dinosaurs [S107] and once were considered to represent Triassic members of the Ornithomimosauria [S136]. We use *Effigia* as a surrogate taxon for the unnamed Otis Chalk shuvosaurid (e.g. TMM 31100-509, right femur; TMM 31100-512, fused ischia) because it represents the most completely known shuvosaurid and shares multiple postcranial synapomorphies (e.g. long ridge on the lateral side of the pubis, large anteromedial tuber of the femur that is hooked posteriorly) of Shuvosauridae with the Otis Chalk taxon [S110].

Malerisaurus langstoni, [S36].

Age range: late Carnian or early Norian, Late Triassic [S48].

Specimen(s) examined: TMM 31099-11, disarticulated but associated partial skeleton, including partial skull (holotype specimen); TMM 31025-268, partial ptergoid; TMM 31025-261, partial pterygoid; TMM 31025-263, holotype left humerus of *Otischalkia elderae*; additional postcranial material at TMM (Nesbitt, Stocker, Parker unpublished data).

Explanation for selection: *Malerisaurus langstoni* was originally considered to be a 'protorosaur' because of the presence of anteroposteriorly elongate cervical vertebrae [S36]. The taxon is included here because it shares elongated cervical vertebrae with early-diverging sauropodomorph (= 'prosauropod') dinosaurs, but has a rather plesiomorphic body plan similar to *Euparkeria* and *Protorosaurus*. We reinterpret the TMM specimens previously attributed to *Otischalkia* and some specimens identified as *Trilophosaurus* as large specimens of *Malerisaurus langstoni* [S46]. Furthermore, it shares a number of apomorphies with *Azendohsaurus madagaskarensis*, including a deep depression on the ventral surface of the parabisphenoid and a ventrally extended posterolateral condyle of the quadrate [S7].

Triopticus primus, this study.

Age range: late Carnian or early Norian, Late Triassic [S48].

Specimen(s) examined: TMM 31100-1030, partial skull (holotype specimen).

Explanation for selection: As described in this paper, *Triopticus primus* possesses greatly thickened elements of the skull roof that give it a 'dome-like' appearance very similar to what is present in pachycephalosaur dinosaurs. However, it differs from dinosaurs in possessing a horizontally oriented basisphenoid and open posttemporal fenestrae.

Angistorhinus alticephalus, sensu [S41].

Age range: late Carnian or early Norian, Late Triassic [S48].

Specimen(s) examined: OMNH 733, partial skull, nine presacral vertebrae, isolated rib fragments, and dermal osteoderms (holotype specimen); TMM 31100-1332, nearly complete skeleton; TMM 31098-1, skull.

Explanation for selection: Phytosaurs are archosauriforms with anteroposteriorly elongate premaxillae that form a distinct rostrum. The rostrum in *Anghistorhinus alticephalus* is relatively narrow with a homodont dentition, which has been suggested to be characteristic of a piscivorous diet (e.g. [S114]). *Angistorhinus alticephalus* is recognized from the Otis Chalk locality by several specimens, including a nearly complete skeleton (TMM 31100-1332), which represents one of the most complete North American phytosaur specimens ever recovered [S46, S137].

Revueltosaurus callenderi, sensu [S138]

Age range: middle to late Norian, Late Triassic [S139].

Specimen(s) examined: PEFO 34561, nearly complete skeleton and skull.

Explanation for selection: *Revueltosaurus* initially was known from isolated, leaf-shaped teeth, and was classified as an ornithischian dinosaur because of that dentition [S106]. However, newly collected partial skeletons have demonstrated that the taxon instead is a pseudosuchian with a heavy carapace and ventral armor similar to aetosaurs [S5, S138].

Longosuchus meadei, sensu [S125]

Age range: late Carnian or early Norian, Late Triassic [S48].

Specimen(s) examined: TMM 31185-98, skull (lectotype specimen); TMM 31185-97, postcranial skeleton and carapace.

Explanation for selection: Aetosaurs are pseudosuchians with leaf-shaped teeth and a heavy armor carapace [S140]. *Longosuchus meadei* from the Otis Chalk locality represents one of the most complete aetosaurs known [S57, S113, S125].

Poposaurus gracilis, sensu [S141]

Age range: Carnian to early Norian, Late Triassic [S139].

Specimen(s) examined: YPM VP 57100, complete articulated skeleton lacking most of the skull; PEFO 34865, partial skull and postcranium.

Explanation for selection: *Poposaurus gracilis* originally was thought to be a dinosaur because of its inferred bipedality, recurved carnivorous dentition, and general theropod-like bauplan (e.g. [S142]). Rather, it is one of the best known poposauroids [S143, S144]. *Poposaurus gracilis* is represented by a well-

preserved ilium from the Otis Chalk assemblage (UMMP 11748) (clear ridge on lateral side of the ilium posterior to the supra-acetabular crest and a ball-in-socket articulation between the ilium and the ischium [S145]).

Eoraptor lunensis, sensu [S146]

Age range: late Carnian, Late Triassic [S4].

Specimen(s) examined: PVSJ 512, nearly complete skeleton with skull (holotype specimen).

Explanation for selection: *Eoraptor lunensis* is an important though controversial taxon for character optimizations at the base of Theropoda and for Saurischia [S147], but now is hypothesized to be one of the earliest diverging sauropodomorphs [S4, S148]. The taxon has leaf-shaped premaxillary and anterior maxillary teeth and an inferred bipedal posture. *Eoraptor* also is noteworthy for the presence of palatal teeth [S148], a rare feature within Dinosauria [S5].

Plateosaurus engelhardti, sensu [S149]

Age range: middle Norian, Late Triassic [S149].

Specimen(s) examined: SMNS 13200, nearly complete skeleton and skull; AMNH FARB 6810, skull and complete skeleton.

Explanation for selection: *Plateosaurus engelhardti* is one of the most well-known Triassic dinosaurs and here is representative of the early sauropodomorph dinosaur bauplan [S5, S150, S151]. Sauropodomorphs such as *Plateosaurus engelhardti* bear leaf-shaped teeth and anteroposteriorly elongate vertebrae [S150, S152, S153] similar to those found in some archosauromorphs.

Coelophysis bauri, sensu [S131]

Age range: late Norian to Rhaetian, Late Triassic [S135].

Specimen(s) examined: AMNH FARB 7224, complete articulated skeleton missing the tail (neotype specimen); AMNH FARB 7223, and any coelophysoid material from the *Coelophysis* Quarry, including CM 31374, a complete skull.

Explanation for selection: *Coelophysis bauri* is one of the best preserved Triassic dinosaurs, representative of early-diverging neotheropods and used extensively in phylogenetic analyses (e.g. [S5, S9, S130]). *Coelophysis* is a gracile, bipedal theropod with recurved teeth [S131].

Jurassic Period

Protosuchus richardsoni, sensu [S154]

Age range: Hettangian, Early Jurassic [S155].

Specimen(s) examined: AMNH FR 3016, crushed skull and nearly complete skeleton (holotype specimen); MCZ 6727, skull and partial skeleton; UCMP 131827, partial skull and skeleton; UCMP 130860, skull; UCMP 36717, postcranial skeleton.

Explanation for selection: *Protosuchus richardsoni* forms part of the definition of Crocodyliformes. This taxon is known by multiple well-preserved specimens and is included in multiple phylogenetic analyses of crocodylian-line archosaurs (e.g. [S156, S157]).

Calsoyasuchus valliceps, sensu [S158]

Age range: Sinemurian to Pliensbachian, Early Jurassic [S158].

Specimen(s) examined: TMM 43631-1, partial skull (holotype specimen).

Explanation for selection: *Calsoyasuchus* is one of the earliest known longirostrine crocodyliforms with pneumatic nasal cavities [S158]. *Calsoyasuchus* is included here because of the general rostral similarities to those of phytosaurs.

Pelagosaurus typus, sensu [S159]

Age range: Toarcian, Early Jurassic [S159].

Specimen(s) examined: BRLSI M1413, well-preserved skull. See additional material listed by Pierce and Benton [S159].

Explanation for selection: Thalattosuchians most recently were found as the earliest appearing group of longirostrine crocodyliforms [S160]. The elongate, narrow rostrum and generally homodont dentition have been suggestive of a piscivorous diet, which was supported by the presence of the fish *Leptolepis* in the rib

cage of an individual [S159]. *Pelagosaurus* is included here because it shares the presence of rostral elongation with phytosaurs and is known by three-dimensionally preserved specimens.

Lesothosaurus diagnosticus, sensu [S161]

Age range: Hettangian-Sinemurian, Early Jurassic [S162].

Specimen(s) examined: NHMUK RUB 17, two disarticulated skeletons including much of a single skull (syntype specimen); NHMUK RUB 23, partial skull and nearly complete disarticulated skull (syntype specimen) [S161].

Explanation for selection: *Lesothosaurus diagnosticus* is one of the basal-most ornithischian dinosaurs [S5, S161, S163] and is known from multiple well preserved cranial and postcranial specimens. It is often included in phylogenetic analyses as a representative early diverging ornithichian (e.g. [S5, S164]), and we additionally include it here because *Lesothosaurus* possesses leaf-shaped teeth similar to those of *Silesaurus* [S5].

Limusaurus inextricabilis [S165]

Age range: Oxfordian, Middle-Late Jurassic [S166].

Specimen(s) examined: IVPP V 15923, articulated and nearly complete skeleton (holotype skeleton); IVPP V 15924, semi-articulated skeleton missing the skull.

Explanation for selection: *Limusaurus inextricabilis* is known by two relatively complete skeletons and previously was recognized to share multiple skeletal features with the distantly-related and temporally-separated ornithomimosaurian dinosaurs and shuvosaurid suchians [S165].

Allosaurus fragilis, sensu [S167]

Age range: Kimmeridgian-Tithonian, Late Jurassic [S168].

Specimen(s) examined: UUVV 6000, complete skull and partial skeleton (neotype specimen) [S169].

Explanation for selection: *Allosaurus fragilis* is an excellent example of a large Jurassic neotheropod dinosaur and is one of the best preserved [S169]. It has been included in several important phylogenetic analyses of the Theropoda (e.g. [S9, S170]).

Cretaceous Period

Baryonyx walkeri, sensu [S171]

Age range: Barremian, Lower Cretaceous [S172].

Specimen(s) examined: NHMUK R9951, much of the skull and postcranium (holotype specimen).

Explanation for selection: *Baryonyx walkeri* is a member of the Spinosauridae, a group of specialized theropod dinosaurs that have an elongated rostral morphology convergent with that of crocodylians [S173]. As in crocodylians, and differing from phytosaurs, the rostrum is mainly comprised by the maxillae; the elongation is a possible adaptation for piscivory [S171, S172, S174]. *Baryonyx walkeri* lacks a dorsal “sail” unlike other spinosaurids such as *Spinosaurus aegyptiacus*.

Spinosaurus aegyptiacus, sensu [S175]

Age range: Cenomanian, Late Cretaceous [S175].

Specimen(s) examined: BSP 1912 VIII 19, mandibular ramus, partial vertebral column (holotype specimen, destroyed in World War II) [S176, S177]; MSNM V4047, anterior portion of rostrum [S175]; FSAC-KK 11888, incomplete skull and partial postcranium (neotype specimen; [S178]).

Explanation for selection: *Spinosaurus aegyptiacus* is a purported piscivorous theropod dinosaur with an elongate rostrum and dorsoventrally elongate neural spines of the trunk vertebrae that formed a pronounced ‘sail’ [S175, S177, S178]. Other spinosaurids are known from more complete materials (e.g. *Suchomimus tenerensis*, [S179]); however, *Spinosaurus aegyptiacus* bears both an elongate rostrum and expanded neural spines [S178, S179], two conditions that are convergent with several Triassic non-dinosaurian archosaurs (e.g. phytosaurs, *Arizonasaurus babbitti*).

Ornithomimus edmontonicus, sensu [S180]

Age range: Campanian, Late Cretaceous [S181].

Specimen(s) examined: RTMP 95.110.1, nearly complete skeleton including complete skull [S180, S182, S183].

Explanation for selection: *Ornithomimus edmontonicus* Sternberg 1933 is best known from a referred nearly complete skeleton and skull (RTMP 95.110.1) that also preserves evidence of soft tissues, making this one of the best preserved ornithomimid dinosaurs [S182]. Ornithomimids are gracile, bipedal theropod dinosaurs with edentulous jaws [S180], features that are convergent with shuvosaurid suchians from the Late Triassic [S107].

Stegoceras validum, sensu [S184]

Age range: Campanian, Late Cretaceous [S185].

Specimen(s) examined: CMN 515, frontoparietal (lectotype specimen); UALVP-2, complete skull [S184, S186].

Explanation for selection: Pachycephalosaurs are ornithischian dinosaurs known from the Late Cretaceous that are characterized by greatly thickened, dome-like skull roofs and a dentition of leaf-shaped teeth (e.g. [S184]). Some of the best-preserved skulls and postcrania are those of *Stegoceras validum* Lambe 1902 (UALVP-2; [S184, S186]). *Stegoceras validum* is included in this study to test convergences with the skull roof of *Triopticus primus*.

Gastonia burgei, sensu [S187]

Age range: Barremian, Early Cretaceous [S188].

Specimen(s) examined: CEUM 1307, skull (holotype specimen); see Kirkland [S187] for list of postcranial elements.

Explanation for selection: *Gastonia burgei* is an early diverging ankylosaurid dinosaur from the Early Cretaceous of Utah that is known from a complete skull and a relatively complete carapace [S187]. The heavy armor and leaf-shaped teeth of ankylosaurs are convergent with Late Triassic suchians such as aetosaurs [S140] and *Revueltosaurus callenderi* [S138].

Sauropelta edwardsorum, sensu [S189]

Age range: Aptian, Early Cretaceous [S188].

Specimen(s) examined: AMNH 3036, partial skeleton lacking the skull (holotype specimen); YPM 5502, mandible with teeth [S189]. See Ostrom [S189] for list of additional specimens.

Explanation for selection: *Sauropelta edwardsorum* is a nodosaurid dinosaur from the Early Cretaceous mainly known from a well-preserved and articulated carapace (AMNH 3036; [S189]). A referred mandible bears 10 leaf-shaped teeth [S189]. The carapace and tooth morphology of nodosaurids are convergent with aetosaurs [S140] and *Revueltosaurus callenderi* [S138] from the Late Triassic.

Quaternary

Gavialis gangeticus, sensu [S190]

Age range: Recent, Quaternary Epoch

Specimen(s) examined: TMM M-5490, skull and partial skeleton.

Explanation for selection: Gavialoids, including the extant Indian gharial *Gavialis gangeticus*, are early-diverging crocodylians (in morphology-based phylogenetic analyses; see [S2, S191]) with an elongate, but narrow rostrum and a homodont dentition [S2]. These adaptations are potentially indicative of a piscivorous diet of *Gavialis* and convergent with the cranial morphologies of some phytosaurs (e.g. [S114]).

List of characters used in convergence analysis

1. Parietal-squamosal shelf: absent (0); present (1). From [S10], character 1 of the Marginocephalia portion of the large dinosaur phylogeny.
2. Supratemporal fenestra orientation: dorsally or nearly dorsally directed (0); laterally directed (1). Modified from [S5], character 143.
3. Supratemporal fenestra, relative size: greater than 1/4 anteroposterior length of orbit (0); less than 1/4 anteroposterior length of orbit or absent (1). New character.
4. Otooccipital, paroccipital process, dorsal margin: separated from ventral margin of squamosal (0); connected to ventral margin of squamosal (1). New character.
5. Supraorbital bones (=palpebrals): absent (0); present (1). Modified from [S5], character 147.
6. Quadrate, long axis of body, angle: posteroventrally or vertically (0); anteroventrally (1). From [S5], character 82.

7. Quadrate, head: partially exposed in lateral view (0); completely covered by the squamosal (1). From [S5, S147, S192-195]; [S19], character 78.
8. Skull roof, dorsal to orbit: thickness similar to the nasals (0); skull roof clearly thickened relative to the nasals (1). Similar to [S196], character 4. Note, the thickened skull roof can include the frontals, frontal and parietal, or the parietal because this character does not focus on the homology of the expansion, just the expansion dorsal to the orbits.
9. Skull roof, dorsal to braincase: flat (0); distinctly vaulted (1). Modified from [S197], character 15.
10. Posterior edge of skull roof, surface texture: generally smooth (0); possessing node-like protuberances (1). Modified from [S197], character 5.
11. Exoccipital, lateral side, metotic strut: absent (0); present (1). Modified from [S72]; [S126], character 77.
12. Parabasisphenoid, ventral surface, midline: flat (0); distinct depression (1). [S5], character 100.
13. Internal carotid arteries, entrance into braincase: ventral (0); lateral (1). Modified from [S5], character 95.
14. Postfrontal: present (0); absent (1). From [S198]; [S5], character 44.
15. Otoccipitals, paroccipital processes, orientation: lateral or posterolateral (0); ventrally deflected (1). Modified from [S5], character 110.
16. Dentary, anterior extremity: rounded (0); tapers to sharp point (1). From [S5], character 155.
17. Dentition: generally homodont (0); markedly heterodont (1). From [S199], character 15.
18. Tooth, serrations: absent (0); present (1). From [S200], listed in diagnosis of Archosauria; [S193], character 3.
19. Tooth, serrations, shape: rectangular or rounded (0); pointed (1). Modified from [S5], character 168.
20. Narial size: clearly smaller diameter than orbit (0); diameter of naris equal to or larger than orbital diameter (1). New character.
21. Rostrum length, measured from anterior border of orbit to tip of premaxilla over total length of skull: preorbital length less than 60% of skull length (0); preorbital length more than 60% of skull length (1). Modified from [S201], character 1.
22. Snout, neurovascular foramina: absent (0); present and densely covering anterior portion of snout (1). New character.
23. Premaxilla, anterior tip: transverse and horizontal (0); downturned (1). Modified from [S202], character 2.
24. Cranial length, relative to presacral vertebral column: less than half the length (0); more than half or greater the length (1). From [S132], character 33.
25. Dentary, anterior tip: deflected slightly ventrally or pointed anteriorly or nearly flat (0); curved dorsally (1). New formulation based on [S5], characters 154 and 155.
26. Narial openings: directed laterally (0); directed dorsally (1). From [S132], character P.
27. Frontal-parietal fusion: absent (0); present (1). New character.
28. Position of external nares: terminal (0); non-terminal, well posterior of the anterior end of the premaxilla (1). From [S201]; [S203], character 2.
29. Tooth, serrations, number: fine, 5 or greater per mm (0); coarse, less than 5 per mm (1). New character.
30. Tooth crown, mesiodistal expansion above root: absent (0); present (1). From [S204].
31. Maxillary/dentary teeth, moderately developed lingual expansion of crown (=cingulum): absent (0); present (1). From [S204].
32. Maxillary and dentary crowns, shape: apicobasally tall and blade-like (0); apicobasally short and subtriangular (1). From [S204].
33. Tooth implantation: free at base of tooth (0); teeth fused to bone of attachment at base (1). From [S5], character 174.
34. Dentary teeth: present along entire length of dentary (0); absent in anterior portion (1); completely absent (2). From [S5], character 166.
35. Teeth, posterior edge: concave or straight (0); convex (1). Modified from [S5], character 15.
36. Premaxillary dentition: present (0); absent (1). From [S107], character 73.
37. Premaxillary teeth and dentary teeth: premaxillary teeth are labial to dentary teeth (0); premaxillary teeth interlock with dentary teeth (1). New character.
38. Maxillary dentition: present (0); absent (1). From [S107], character 74.
39. Mandibular fenestra: absent (0); present and less than half the length of the mandible (1); present and equal to more than half the length of the mandible (2). Modified from [S107], character 77.

40. Anterior cervical centra, length versus height: length greater than height (0); length and height subequal (1); length much shorter than height (2). Modified from [S205], character 26.
41. Cervical vertebrae, rimmed depression on posterior part of centrum: absent (0); present (1). From [S5], character 189.
42. Posterior cervical vertebrae, diapophysis, posteriorly directed processes: absent (0); present (1). Discussed by [S110].
43. Posterior trunk (=dorsal) vertebrae, transverse processes: shorter than or equal to the length of the centrum (0); longer than the length of the centrum (1). New character.
44. Presacral vertebrae, neural spines, dorsal margin: unexpanded (0); laterally expanded into a platform (=spine table) (1). Modified from [S5], characters 191 and 197.
45. Sacral vertebrae, total number: 2 (0); more than 2 (1). Modified from [S10], character 6 of the Dinosauria portion of the large dinosaur phylogeny.
46. Sacrum, neural spines: not fused (0); fused (1). From [S110], character 82.
47. Sacral vertebrae, centra articular rims: present in the sacrum (0); nearly obliterated, fused into a rod-like structure (1). From [S110]; [S5], character 204.
48. Distal caudal vertebrae, prezygapophyses: not elongated (0); elongated more than one-quarter the length of adjacent centrum (1). Modified from [S198], character 20.
49. Epipophyses: absent in postaxial anterior cervical vertebrae (0); present in postaxial anterior cervical vertebrae (1). From [S5], character 186.
50. Postaxial intercentra: present (0); absent (1). From [S5], character 177.
51. Hyposphene-hypantrum articulations in the presacral vertebrae: absent (0); present (1). From [S198], character 6.
52. Scapula, blade, distal end: expanded anteriorly and/or posterior or unexpanded relative to the midpoint of the blade (0); tapered (1). Modified from [S198], character 41.
53. Humerus, proximal portion: expanded more than twice the width of the midshaft of the humerus (0); expanded less than or equal to twice the width of the midshaft of the humerus (1). From [S5], character 236.
54. Humerus, distal end width: narrower or equal to 30% of humerus length (0); greater than 30% of humerus length (1). From [S5], character 235.
55. Ulna, olecranon process: absent or poorly developed (0); well-developed (1). New character.
56. Manus, size: about 1/5 or more the length of the pes (0); highly reduced, less than 1/5 the length of the pes (1). New character.
57. Manual unguals, length: about the same length or shorter than the last phalanx of same digit (0); distinctly longer than last phalanx of same digit (1). From [S7], character 222.
58. Ilium, anterior portion of blade, cuppedicus fossa: absent (0); present (1). From [S9]; discussed by [S110].
59. Ilium, anterior process: short and does not extend anterior to the acetabulum (0); long and extends anterior to the acetabulum (1). Modified from [S5], character 269.
60. Ilium, posterior portion of blade, ventral view, brevis fossa: absent (0); present (1). Modified from [S194], character 26.
61. Ilium, acetabulum: directed laterally or deflected up to 60 degrees ventral of mediolateral (0); directed more than 60 degrees of mediolateral (1). Modified from [S5], character 270.
62. Ilium, ventral margin, within acetabulum: convex or straight (0); concave (1). Modified from [S5], character 273.
63. Pubis, length: shorter than the anteroposterior length of the blade of the ilium (0); longer than the anteroposterior length of the blade of the ilium (1). New character.
64. Pubis, distal end: tapers or no expansion (0); posteriorly expanded into boot and length of the expansion less than 30% the length of the shaft (1); posteriorly expanded into boot and length of the expansion greater than 30% the length of the shaft (2). Modified from [S5], characters 283 and 285.
65. Pubis, length: equal or subequal in length to the ischium (0); longer than ischium (1). From [S5], character 282.
66. Ischium, distal end: unexpanded or tapers (0); expanded ventral relative to the ischial shaft (=ischial boot) (1). From [S5], character 294.
67. Femur length relative to tibia length: femur longer than tibia length (0); tibia longer than or equal to femur length (1). From [S5], character 299.

68. Femur, anteromedial portion: continuous with femoral shaft (0); posteriorly hooked (=offset femoral head) (1). New formulation from [S198], character 45 in Appendix A.
69. Femur, bone wall thickness at or near midshaft: thickness/diameter >0.3 (0); thin thickness/diameter < 0.3 (1). From [S5], character 323.
70. Tibia, proximal portion expansion, longest dimension: shorter than 35% the length of the tibia (0); longer than 35% the length of the tibia (1). New character.
71. Tibia, lateral side, proximal half, proximodistally-oriented crest (=fibular crest): absent (0); present (1). From [S5], character 333.
72. Astragalus, anterior portion of proximal surface, anterior ascending process: absent (0); present (1). Modified from [S198], character 48 in Appendix A.
73. Calcaneum size: about the same size of the astragalus or slightly smaller (0); reduced to a small cube-like structure, much smaller than that of the astragalus (1). Modified from [S198], character 48 in Appendix A.
74. Calcaneum, calcaneal tuber: present (0); absent (1). From [S198].
75. Pes, longest metatarsal: 4 (0); 3 (1). Modified from [S206], character 95.
76. Pes, metatarsal I, length: longer than or equal to half the length of metatarsal II (0); shorter than half the length of metatarsal II (1). Modified from [S10], character 142 of the Dinosauria portion of the large dinosaur phylogeny.
77. Pes, digit 5, number of phalanges: 1 or more (0); zero (1). Modified from [S5], character 399.
78. Pes, ungual, shape: weakly mediolaterally compressed or triangular in cross section (0); strongly dorsoventrally compressed (1); strongly mediolaterally compressed with a sharp dorsal ridge (2). Modified from [S5], character 400.
79. Osteoderms: absent (0); present (1). From [S207], character 57.
80. Osteoderms, arrangement: one column of paramedian osteoderms on either side of midline (0); two or more columns (paramedian and lateral) of osteoderms on either side of midline (1); second column elongated and recurved into spikes (2). Modified from [S5], character 406.
81. Forelimb-hindlimb length ratio: more than 0.55(0); less than 0.55(1). From [S5], character 212. This character is essentially a proxy for quadrupedalism (state 0) and bipedalism (state 1) [S143].

Detailed results of the convergence analyses

Our nMDS analyses resulted in a broad overlap of non-archosaurian archosauromorphs and archosaur taxa across all coordinates for both the analysis of total bauplan convergence (cranial and postcranial characters) and the analysis focused only on cranial characters (Fig. 3). Specifically, we identify pockets of convergence in morphospace occupation in dome-headed taxa, long-snouted taxa, armored taxa, bipedal carnivorous taxa, beaked taxa, and a group of taxa with a plesiomorphic bauplan. In the ordination plots based on the total bauplan, *Triopticus* occupies a position relatively far from other taxa in the analysis; however, the taxon closest to *Triopticus* in several plots of total bauplan morphospace is *Stegoceras*, the pachycephalosaur (Fig. 3; Fig. S3A, B), and the two taxa group together in a cluster analysis for total bauplan (Fig. S3C). Both of these taxa share several features related to the expansion and thickening of the skull roof (e.g. convergence characters 1, 8, 9). The ordination distances and observed dissimilarity were highly correlated, with an R^2 of 0.979 for the analysis of total bauplan convergence (see the Shepard plot in Fig. S3D [S208]), and the analyses resulted in a stress of 0.0684 (see Table S1).

In the nMDS analysis using cranial characters only, *Stegoceras* is not positioned as closely to *Triopticus* as in the analysis including all characters (Fig. 3B, S3E, F) When axis 2 is plotted against axis 3, morphospace is more evenly occupied, with *Triopticus* positioned closer to both Triassic and post-Triassic taxa such as *Malerisaurus*, *Baryonyx*, and *Pelagosaurus* (Fig. S3F). Additionally, *Triopticus* and *Stegoceras* do not group together in the cluster analysis based on cranial characters (Fig. S3G). The analysis including only cranial characters yielded a similarly high R^2 of 0.973, with a stress value of 0.0717 (Fig. S3H; see Table S2 for convergence scores).

Among our groupings are several well-known examples of convergence between Triassic non-dinosaurian archosaurs and dinosaurs or other post-Triassic taxa. In the total bauplan analysis, *Effigia*, *Ornithomimus*, and *Limusaurus*, taxa that all share bipedal postures, large orbits, and are either edentulous or have dramatically reduced dentition either cluster together tightly (Fig. 3A), or are positioned relatively close together (Fig. S3B). However, their distributions are more integrated with other Triassic archosaurs such as *Plateosaurus* and *Asilisaurus*, as well as *Protosuchus*, and *Allosaurus* when axis 1 is plotted against

axis 3 (Fig S3A). In the analysis restricted to cranial characters, *Effigia*, *Ornithomimus*, and *Limusaurus* again group together in several plots (Fig. 3B; Fig. S3E, F). In the cluster analyses for both cranial and total bauplan characters, *Effigia*, *Ornithomimus*, and *Limusaurus* all group together, reinforcing their close morphological similarity.

Long-snouted taxa such as *Angistorhinus*, *Pelagosaurus*, *Gavialis*, and, to a degree, *Spinosaurus* and *Baryonyx*, cluster together in the full-body analysis, but are mixed with other taxa (Fig 3A; Fig. S3A, B), whereas this relationship is clearer in the cranial-only dataset (Fig. 3B; Fig. S3E, F). However, *Calsoyasuchus* is further from this main 'long snouted' grouping. The impact of postcrania on the grouping of these 'long snouted' taxa is evident when comparing results of the cluster analyses of all characters and cranial characters only: *Calsoyasuchus*, *Pelagosaurus*, *Gavialis*, *Baryonyx*, *Spinosaurus*, and *Angistorhinus* all group together in the cranial-only cluster analysis (Fig. S3G), while they are more spread out in the analysis including all characters (Fig. S3C).

We also recover several groupings based on convergence in post-cranial characters. Carnivorous taxa with bipedal postures, such as *Allosaurus*, *Spinosaurus*, *Baryonyx*, and *Coelophysis*, group together in the full-body analysis (Fig. 3A), but the positions of these taxa are more spread out in the cranial-only analysis (Fig. 3B; Fig. S3E, F). These relationships are reflected in the cluster analyses, where all four taxa cluster together in the analysis including all characters (Fig. S3C), but group with other taxa in the cranial-only analysis (Fig. S3G). A grouping of armored taxa (the aetosaur *Longosuchus* and dinosaurs *Gastonia* and *Sauropelta*) also is recovered in the total-body analysis (Fig. 3A; Fig. S3A, B), but these taxa are widely dispersed throughout morphospace when only cranial characters are used (Fig 3B; Fig. S3E, F). Again, the cluster analysis using all characters recovers this grouping (Fig. S3C), but it is lost in the cranial-only analysis (Fig. S3G). Lastly, plesiomorphic taxa like *Prolacerta*, *Protosuchus*, *Euparkeria*, and *Protorosaurus* group together in several plots from the full-body dataset (Fig. 3A; Fig. S3B), and this relationship also can be seen in several plots from the cranial-only dataset (Fig. 3B; Fig. S3G), but is not as clear in the plot of axis 1 versus 3 (Fig. S3E). Overall, the analysis including both cranial and postcranial characters shows tighter groupings of taxa in which the convergence mainly occurs in the postcranial skeleton (body armor, bipedalism, or a general plesiomorphic bauplan) and the analysis using cranial characters only shows tighter groupings for convergence in characters related to the head (dome-headed taxa, long-snouted taxa). These results underscore the importance of dataset partitioning, and evaluating the differences in signal coming from those partitions.

As one final test, we ran the same nMDS analysis using all archosauromorph taxa known from the Otis Chalk assemblage, even though not all of them have post-Triassic morphological correlates (Fig. S4; see Table S3 for convergence scores). These additional taxa were *Trilophosaurus* (based on TMM 31185-140), *Azendohsaurus* (as another taxon potentially closely-related to *Malerisaurus*; based on [S7, S105]), *Doswellia* (USNM 244214; TMM 31025-152), and an unnamed loricatan (TMM 31098-46). Many of the relationships we observed in previous analyses are retained in this analysis as well, including the grouping of *Triopticus* and *Stegoceras* (Fig. S4A, C) beaked taxa (*Effigia*, *Ornithomimus*, and *Limusaurus*; Fig. S4B, C), armored taxa (*Longosuchus*, *Sauropelta*, and *Gastonia*; Fig. S4A, C), long-snouted taxa (*Angistorhinus*, *Pelagosaurus*, *Gavialis*, and *Baryonyx*; Fig. S4A, C), and bipedal carnivores (*Allosaurus*, *Spinosaurus*, *Baryonyx*, and *Coelophysis*; Fig. S4C). The stress was similar to previous analyses, at 0.0723, and the ordination distance again is tightly correlated with observed dissimilarity, at 0.982 (Fig. S4D). Some of the relationships recovered in the nMDS plots are preserved in the cluster analysis, including clusters of beaked taxa, bipedal carnivores, and armored taxa (Fig. S4E). Despite preservation of some of the groupings of convergent morphologies, taxa in this analysis are more tightly grouped overall than in previous analyses, forming large clusters (Fig. S4A, C). The newly added taxa seem to be interspersed throughout the morphospace, positioned among other taxa in these large groupings (Fig. S4A-C).

Supplemental References

- S1. Arbour, V.M., and Currie, P.J. (2015). Systematics, phylogeny and palaeobiogeography of the ankylosaurid dinosaurs. *Journal of Systematic Palaeontology*, 1-60.
- S2. Brochu, C.A. (1997). Morphology, fossils, divergence timing, and the phylogenetic relationships of *Gavialis*. *Systematic Biology* 46, 479-522.
- S3. Dilkes, D., and Sues, H.-D. (2009). Redescription and phylogenetic relationships of *Doswellia kaltenbachi* (Diapsida: Archosauriformes) from the Upper Triassic of Virginia. *Journal of Vertebrate Paleontology* 29, 58-79.

- S4. Martinez, R.N., Sereno, P.C., Alcober, O.A., Colombi, C.E., Renne, P.R., Montañez, I.P., and Currie, B.S. (2011). A basal dinosaur from the dawn of the dinosaur era in southwestern Pangaea. *Science* 331, 206-210.
- S5. Nesbitt, S.J. (2011). The early evolution of archosaurs: relationships and the origin of major clades. *Bulletin of the American Museum of Natural History* 352, 1-292.
- S6. Nesbitt, S.J., and Ezcurra, M.D. (2015). The early fossil record of dinosaurs in North America: a new neotheropod (Dinosauria: Theropoda) from the base of the Dockum Group (Upper Triassic) of Texas. *Acta Palaeontologica Polonica* 60, 513-526.
- S7. Nesbitt, S.J., Flynn, J.J., Pritchard, A.C., Parrish, J.M., Ranivoharimanana, L., and Wyss, A.R. (2015). Postcranial osteology of *Azendohsaurus madagaskarensis* (?Middle to Upper Triassic, Isalo Group, Madagascar) and its systematic position among stem archosaur reptiles. *Bulletin of the American Museum of Natural History* 899, 1-125.
- S8. Pol, D., Turner, A.H., and Norell, M.A. (2009). Morphology of the Late Cretaceous crocodylomorph *Shamosuchus djadochtaensis* and a discussion of neosuchian phylogeny as related to the origin of Eusuchia. *Bulletin of the American Museum of Natural History* 324, 1-103.
- S9. Rauhut, O.W.M. (2003). The interrelationships and evolution of basal theropod dinosaurs. *Special Papers in Palaeontology* 69, 1-213.
- S10. Sereno, P.C. (1999). The evolution of dinosaurs. *Science* 284, 2137-2147.
- S11. Witmer, L.M., Chatterjee, S., Franzosa, J., and Rowe, T. (2003). Neuroanatomy of flying reptiles and implications for flight, posture and behaviour. *Nature* 425, 950-953.
- S12. Witmer, L.M., Ridgely, R.C., Dufeu, D.L., and Semones, M.C. (2008). Using CT to peer into the past: 3D visualization of the brain and ear regions of birds, crocodiles, and nonavian dinosaurs. In *Anatomical Imaging: Towards a New Morphology*, H. Endo and R. Frey, eds. (Tokyo: Springer-Verlag), pp. 67-88.
- S13. Vickaryous, M.K., Russell, A.P., and Currie, P.J. (2001). The cranial ornamentation of ankylosaurs (Ornithischia: Thyreophora): reappraisal of developmental hypotheses. In *The Armored Dinosaurs*, K. Carpenter, ed. (Bloomington: Indiana University Press), pp. 318-340.
- S14. Camp, C.L. (1930). A study of the phytosaurs with description of new material from western North America. *Memoirs of the University of California* 10, 1-174.
- S15. Case, E.C. (1921). On an endocranial cast from a reptile, *Desmotosuchus spurensis*, from the Upper Triassic of western Texas. *Journal of Comparative Neurology* 33, 133-147.
- S16. Case, E.C. (1928). An endocranial cast of a phytosaur from the Upper Triassic beds of western Texas. *Journal of Comparative Neurology* 45, 161-168.
- S17. Chatterjee, S. (1978). A primitive parasuchid (Phytosaur) reptile from the Upper Triassic Maleri Formation of India. *Palaentology* 21, 83-127.
- S18. Holloway, W.L., Claeson, K.M., and O'Keefe, F.R. (2013). A virtual phytosaur endocast and its implications for sensory system evolution in archosaurs. *Journal of Vertebrate Paleontology* 33, 848-857.
- S19. Hopson, J.A. (1979). Paleoneurology. In *Biology of the Reptilia*. Neurology A, Volume 9, C. Gans, R.G. Northcutt and P.S. Ulinki, eds. (New York: Academic Press), pp. 39-146.
- S20. Bourke, J.M., Porter, W.R., Ridgely, R.C., Lyson, T.R., Schachner, E.R., Bell, P.R., and Witmer, L.M. (2014). Breathing life into dinosaurs: tackling challenges of soft-tissue restoration and nasal airflow in extinct species. *Anatomical Record* 297, 2148-2186.
- S21. Balanoff, A.M., Bever, G.S., and Norell, M.A. (2014). Reconsidering the avian nature of the oviraptorosaur brain (Dinosauria: Theropoda). *PLoS ONE* 9, e113559.
- S22. Balanoff, A.M., Bever, G.S., Rowe, T.B., and Norell, M.A. (2013). Evolutionary origins of the avian brain. *Nature* 501, 93-96.
- S23. Witmer, L.M., and Ridgely, R.C. (2009). New insights into the brain, braincase, and ear region of tyrannosaurs, with implications for sensory organization and behavior. *Anatomical Record* 292, 1266-1296.
- S24. Borsuk-Białynicka, M., and Evans, S.E. (2009). Cranial and mandibular osteology of the Early Triassic archosauriform *Osmolskina czatkowicensis* from Poland. *Palaeontologia Polonica* 65, 235-281.
- S25. Gower, D.J. (1997). The braincase of the early archosaurian reptile *Erythrosuchus africanus*. *Journal of Zoology (London)* 242, 557-576.

- S26. Gower, D.J., and Weber, E. (1998). The braincase of *Euparkeria*, and the evolutionary relationships of birds and crocodylians. *Biological Review* 73, 367-411.
- S27. Voogd, J., and Wylie, D.R. (2004). Functional and anatomical organization of floccular zones: a preserved feature in vertebrates. *Journal of Comparative Neurology* 470, 107-112.
- S28. Romer, A.S. (1956). *Osteology of the Reptiles*, (Chicago: University of Chicago Press).
- S29. Butler, A.B., and Hodos, W. (2005). *Comparative Vertebrate Neuroanatomy. Evolution and Adaptation*, 2nd Edition, (Hoboken: John Wiley and Sons).
- S30. Quay, W.B. (1979). The parietal eye-pineal complex. In *Biology of the Reptilia*, Volume 9, C. Gans, ed. (New York: Academic Press), pp. 245-406.
- S31. Cassone, V.M., and Kumar, V. (2014). Circadian Rhythms. In *Sturkie's Avian Physiology*, 6th Edition, C.G. Scanes, ed. (Amsterdam: Elsevier (Academic Press)), pp. 811-828.
- S32. Sampson, S.D., and Witmer, L.M. (2007). Craniofacial anatomy of *Majungasaurus crenatissimus* (Theropoda: Abelisauridae) from the Late Cretaceous of Madagascar. *Memoirs of the Society of Vertebrate Paleontology* 8, *Journal of Vertebrate Paleontology* 27, 32-102.
- S33. Georgi, J.A., Sipla, J.S., and Forster, C.A. (2013). Turning semicircular canal function on its head: dinosaurs and a novel vestibular analysis. *PLoS ONE* 8, e58517.
- S34. Hullar, T.E. (2006). Semicircular canal geometry, afferent sensitivity, and animal behavior. *Anatomical Record* 288, 466-472.
- S35. Case, E.C. (1922). New reptiles and stegocephalians from the Upper Triassic of western Texas. *Carnegie Institute of Washington Publication* 321, 1-84.
- S36. Chatterjee, S. (1986). *Malerisaurus langstoni*, a new diapsid reptile from the Triassic of Texas. *Journal of Vertebrate Paleontology* 6, 297-312.
- S37. Gregory, J.T. (1945). *Osteology and relationships of Trilophosaurus*. University of Texas Publication 4401, 273-359.
- S38. Parks, P. (1969). Cranial anatomy and mastication of the Triassic reptile *Trilophosaurus*. (Austin: University of Texas at Austin), p. 89.
- S39. Sawin, H.J. (1945). Amphibians from the Dockum Triassic of Howard County, Texas. The University of Texas Publication 4401, 361-399.
- S40. Schaeffer, B. (1967). Late Triassic fishes from the western United States. *Bulletin of the American Museum of Natural History* 135, 285-342.
- S41. Stovall, J.W., and Wharton, J.B., Jr. (1936). A new species of phytosaur from Big Spring, Texas. *The Journal of Geology* 44, 183-192.
- S42. Wilson, J.A. (1948). A small amphibian from the Triassic of Howard County, Texas. *Journal of Paleontology* 22, 359-361.
- S43. Elder, R.L. (1978). Paleontology and paleoecology of the Dockum Group, Upper Triassic, Howard County, Texas. Volume MS. (Austin: University of Texas), p. 206.
- S44. Elder, R.L. (1987). Taphonomy and paleoecology of the Dockum Group, Howard County, Texas. *Journal of the Arizona-Nevada Academy of Science* 22, 85-94.
- S45. Eberth, D.A., Shannon, M., and Noland, B.G. (2007). A bonebeds database: classification, biases, and patterns of occurrence. In *Bonebeds: genesis, analysis, and paleobiological significance*, R.R. Rogers, D.A. Eberth and A.R. Fiorillo, eds. (Chicago: University of Chicago Press), pp. 103-219.
- S46. Stocker, M.R. (2013). Contextualizing vertebrate faunal dynamics: New perspectives from the Triassic and Eocene of western North America. In *Department of Geological Sciences*, Volume Ph.D. (Austin: The University of Texas at Austin), p. 297.
- S47. Lucas, S.G. (2010). The Triassic timescale based on nonmarine tetrapod biostratigraphy and biochronology. *Geological Society of London Special Publication* 334, 447-500.
- S48. Lucas, S.G., Hunt, A.P., and Kahle, R. (1993). Late Triassic vertebrates from the Dockum Formation near Otis Chalk, Howard County, Texas. *New Mexico Geological Society Bulletin* 44, 237-244.
- S49. Butler, R.J. (2013). '*Francosuchus' trauthi* is not *Paleorhinus*: implications for Late Triassic vertebrate biostratigraphy. *Journal of Vertebrate Paleontology* 33, 858-864.
- S50. Butler, R.J., Rauhut, O.W.M., Stocker, M.R., and Bronowicz, R. (2014). Redescription of the phytosaurs *Paleorhinus* ('*Francosuchus*') *angustifrons* and *Ebrachosuchus neukami* from Germany, with implications for Late Triassic biochronology. *Zoological Journal of the Linnean Society* 170, 155-208.

- S51. Stocker, M.R. (2013). A new taxonomic arrangement for *Paleorhinus scurriensis*. *Earth and Environmental Science Transactions of the Royal Society of Edinburgh* 103.
- S52. Parker, W.G., and Martz, J.W. (2011). The Late Triassic (Norian) Adamanian-Revueltian tetrapod faunal transition in the Chinle Formation of Petrified Forest National Park, Arizona. *Earth and Environmental Science Transactions of the Royal Society of Edinburgh* 101, 231-260.
- S53. Atchley, S.C., Nordt, L.C., Dworkin, S.I., Ramezani, J., Parker, W.G., Ash, S.R., and Bowring, S.A. (2013). A linkage among Pangean tectonism, cyclic alluviation, climate change, and biologic turnover in the Late Triassic: the record from the Chinle Formation, southwestern United States. *Journal of Sedimentary Research* 83, 1147-1161.
- S54. Ramezani, J., Fastovsky, D.E., and Bowring, S.A. (2014). Revised chronostratigraphy of the lower Chinle Formation strata in Arizona and New Mexico (USA): high-precision U-Pb geochronological constraints on the Late Triassic evolution of dinosaurs. *American Journal of Science* 314, 981-1008.
- S55. Fraser, N., Heckert, A., Lucas, S., and Schneider, V. (2006). The first record of *Coahomasuchus* (Archosauria: Stagonolepididae) from the Carnian of eastern North America. *Journal of Vertebrate Paleontology* 26, 63A.
- S56. Heckert, A.B., Schneider, V.P., Fraser, N.C., and Webb, R.A. (2015). A new aetosaur (Archosauria, Suchia) from the Upper Triassic Pekin Formation, Deep River Basin, North Carolina, USA, and its implications for early aetosaur evolution. *Journal of Vertebrate Paleontology* 35, e881831.
- S57. Parker, W.G., and Martz, J.W. (2010). Using positional homology in aetosaur (Archosauria: Pseudosuchia) osteoderms to evaluate the taxonomic status of *Lucasuchus hunti*. *Journal of Vertebrate Paleontology* 30, 1100-1108.
- S58. Whiteside, J.H., Grogan, D.S., Olsen, P.E., and Kent, D.V. (2011). Climatically driven biogeographic provinces of Late Triassic tropical Pangea. *Proceedings of the National Academy of Sciences* 108, 8972-8977.
- S59. LeTourneau, P.M. (2003). Tectonic and climatic controls on the stratigraphic architecture of the Late Triassic Taylorsville Basin, Virginia and Maryland. In *The Great Rift Valleys of Pangea in Eastern North America, Volume 2: Sedimentology, Stratigraphy, and Paleontology*, P.M. LeTourneau, ed. (New York: Columbia University Press), pp. 12-58.
- S60. Olsen, P.E., and Kent, D.V. (1999). Long-period Milankovitch cycles from the Late Triassic and Early Jurassic of eastern North America and their implications for the calibration of the Early Mesozoic time-scale and the long-term behaviour of the planets. *Philosophical Transactions of the Royal Society of London, Series A* 357, 1761-1786.
- S61. Weems, R.E. (1980). An unusual newly discovered archosaur from the Upper Triassic of Virginia, U.S.A. *Transactions of the American Philosophical Society* 70, 1-53.
- S62. Hüsing, S.K., Deenen, M.H.L., Koopmans, J.G., and Krijgsman, W. (2011). Magnetostratigraphic dating of the proposed Rhaetian GSSP at Steinbergkogel (Upper Triassic, Austria): implications for the Late Triassic time scale. *Earth and Planetary Science Letters* 302, 203-216.
- S63. Muttoni, G., Kent, D.V., Olsen, P.E., Di Stefano, P., Lowrie, W., Bernasconi, S.M., and Hernandez, F.M. (2004). Tethyan magnetostratigraphy from Pizzo Mondello (Sicily) and correlation to the Late Triassic Newark astrochronological polarity time scale. *Geological Society of America Bulletin* 116, 1043-1058.
- S64. Ogg, J.G. (2012). Triassic. In *The Geologic Time Scale*, F.M. Gradstein, J.G. Ogg, M.D. Schmitz and G.M. Ogg, eds. (Amsterdam: Elsevier), pp. 681-730.
- S65. Pritchard, A.C., Turner, A.H., Nesbitt, S.J., Irmis, R.B., and Smith, N.D. (2015). Late Triassic tanystropheid (Reptilia, Archosauromorpha) remains from northern New Mexico (Petrified Forest Member, Chinle Formation): insights into distribution, morphology, and paleoecology of Tanystropheidae. *Journal of Vertebrate Paleontology*, 10.1080/02724634.02722014.02911186.
- S66. Brusatte, S.L., Nesbitt, S.J., Irmis, R.B., Butler, R.J., Benton, M.J., and Norell, M.A. (2010). The origin and early radiation of dinosaurs. *Earth-Science Reviews* 101, 68-100.
- S67. Spielmann, J.A., Lucas, S.G., Heckert, A.B., Rinehart, L.F., and Richards, H.R., III (2009). Redescription of *Spinosuchus caseanus* (Archosauromorpha: Trilophosauridae) from the Upper Triassic of North America. *Palaeodiversity* 2, 283-313.
- S68. Goloboff, P., Farris, J., and Nixon, K. (2008). TNT: a free program for phylogenetic analysis. *Cladistics* 24, 774-786.

- S69. Fraser, N.C., and Rieppel, O. (2006). A new protorosaur (Diapsida) from the Upper Buntsandstein of the Black Forest, Germany. *Journal of Vertebrate Paleontology* 26, 866-871.
- S70. Gauffre, F. (1993). The prosauropod dinosaur *Azendohsaurus laaroussii* from the Upper Triassic of Morocco. *Palaeontology* 36, 897-908.
- S71. Gower, D.J. (1999). The cranial and mandibular osteology of a new rauisuchian archosaur from the Middle Triassic of southern Germany. *Stuttgarter Beiträge zur Naturkunde, Serie B* 280, 1-49.
- S72. Gower, D.J. (2002). Braincase evolution in suchian archosaurs (Reptilia: Diapsida): Evidence from the rauisuchian *Batrachotomus kupferzellensis*. *Zoological Journal of the Linnean Society* 136, 49-76.
- S73. Gower, D.J., and Schoch, R. (2009). Postcranial anatomy of the rauisuchian archosaur *Batrachotomus kupferzellensis*. *Journal of Vertebrate Paleontology* 29, 103-122.
- S74. Ezcurra, M.D., and Butler, R.J. (2014). Taxonomy of the proterosuchid archosauriforms (Diapsida: Archosauromorpha) from the earliest Triassic of South Africa, and implications for the early archosauriform radiation. *Palaeontology*, 10.1111/pala.12130.
- S75. Young, C.C. (1978). On a new *Chamatosaurus* from Sinkiang. *Bulletin of the Geological Society of China* 15, 291-320.
- S76. Gower, D.J. (2003). Osteology of the early archosaurian reptile *Erythrosuchus africanus* Broom. *Annals of the South African Museum* 110, 1-84.
- S77. Ewer, R.F. (1965). The anatomy of the thecodont reptile *Euparkeria capensis* Broom. *Philosophical Transactions of the Royal Society of London, Series B* 248, 379-435.
- S78. Evans, S.E. (1980). The skull of a new eosuchian reptile from the Lower Jurassic of South Wales. *Zoological Journal of the Linnaean Society* 70, 203-264.
- S79. Evans, S.E. (1981). The postcranial skeleton of the Lower Jurassic eosuchian *Gephyrosaurus bridensis*. *Zoological Journal of the Linnaean Society* 73, 81-116.
- S80. Saller, F., Renesto, S., and Dalla Vecchia, F.M. (2013). First record of *Langobardisaurus* (Diapsida, Protorosauria) from the Norian (Late Triassic) of Austria, and a revision of the genus. *Neues Jahrbuch für Geologie und Paläontologie Abhandlungen* 268, 83-95.
- S81. Peyer, B. (1937). Die Triasfauna der Tessiner Kalkalpen XII. *Macrocnemus bassanii* Nopcsa. *Abhandlungen der Schweizerischen Palaeontologischen Gesellschaft* 59, 1-140.
- S82. Dilkes, D.W. (1998). The Early Triassic rhynchosaur *Mesosuchus browni* and the interrelationships of basal archosauromorph reptiles. *Philosophical Transactions of the Royal Society of London Series B* 353, 501-541.
- S83. Reisz, R. (1981). A diapsid reptile from the Pennsylvanian of Kansas. *Special Publication of the Museum of Natural History, University of Kansas* 7, 1-74.
- S84. Modesto, S.P., and Sues, H.-D. (2004). The skull of the Early Triassic archosauromorph reptile *Prolacerta broomi* and its phylogenetic significance. *Zoological Journal of the Linnean Society* 140, 335-351.
- S85. Cruickshank, A.R.I. (1972). The proterosuchian thecodonts. In *Studies In Vertebrate Evolution*, K.A. Joysey and T.S. Kemp, eds. (Edinburgh: Oliver and Boyd), pp. 89-119.
- S86. Hughes, B. (1963). The earliest archosaurian reptiles. *South African Journal of Science* 59, 221-241.
- S87. Welman, J. (1998). The taxonomy of the South African proterosuchids (Reptilia, Archosauromorpha). *Journal of Vertebrate Paleontology* 18, 340-347.
- S88. Gottmann-Quesada, A., and Sander, P.M. (2009). Redescription of the early archosauromorph *Protorosaurus speneri* Meyer, 1832, and its phylogenetic relationships. *Palaeontographica Abteilung A* 287, 123-220.
- S89. Benton, M.J. (1990). The species of *Rhynchosaurus*, a rhynchosaur (Reptilia, Diapsida) from the Middle Triassic of England. *Philosophical Transactions of the Royal Society B: Biological Sciences* 328, 213-306.
- S90. Bever, G.S., Bell, C.J., and Maisano, J.A. (2005). The ossified braincase and cephalic osteoderms of *Shinisaurus crocodilurus* (Squamata, Shinisauridae). *Paleaeontologica Electronica* 8, 1-36.
- S91. Conrad, J.L. (2004). Skull, mandible, and hyoid of *Shinisaurus crocodilurus* (Squamata: Anguimorpha). *Zoological Journal of the Linnaean Society* 141, 399-434.
- S92. Conrad, J.L. (2006). Postcranial skeleton of *Shinisaurus crocodilurus* (Squamata: Anguimorpha). *Journal of Morphology* 267, 759-775.

- S93. Nosotti, S. (2007). *Tanystropheus longobardicus* (Reptilia, Protorosauria): re-interpretations of the anatomy based on new specimens from the Middle Triassic of Besano (Lombardy, northern Italy). *Memoire della Civico di Storia Naturale di Milano* 35, 1-88.
- S94. Wild, R. (1973). Die Triasfauna der Tessiner Kalkalpen XXII. *Tanystropheus longobardicus* (Bassani). *Schweizerische Paläontologische Abhandlungen* 95, 1-162.
- S95. Montefeltro, F.C., Bittencourt, J.S., Langer, M.C., and Schultz, C.L. (2013). Postcranial anatomy of the hyperodapedontine rhynchosaur *Teyumbaita sulcognathus* (Azevedo and Schultz, 1987) from the Late Triassic of southern Brazil. *Journal of Vertebrate Paleontology* 33, 67-84.
- S96. Montefeltro, F.C., Langer, M.C., and Schultz, C.L. (2010). Cranial anatomy of a new genus of hyperodapedontine rhynchosaur (Diapsida, Archosauromorpha) from the Upper Triassic of southern Brazil. *Earth and Environmental Science Transactions of the Royal Society of Edinburgh* 101, 27-52.
- S97. Sues, H.-D. (2003). An unusual new archosauromorph reptile from the Upper Triassic Wolfville Formation of Nova Scotia. *Canadian Journal of Earth Sciences* 40, 635-649.
- S98. Spielmann, J.A., Lucas, S.G., Rinehart, L.F., and Heckert, A.B. (2008). The Late Triassic archosauromorph *Trilophosaurus*. *New Mexico Museum of Natural History and Science Bulletin* 43, 1-177.
- S99. El-Toubi, M.R. (1949). The post-cranial osteology of the lizard, *Uromastix aegyptia* (Forskål). *Journal of Morphology* 84, 281-292.
- S100. Currie, P.J. (1981). The vertebrae of *Youngina* (Reptilia: Eosuchia). *Canadian Journal of Earth Sciences* 18, 815-818.
- S101. Gardner, N.M., Holliday, C.M., and O'Keefe, F.R. (2010). The braincase of *Youngina capensis* (Reptilia, Diapsida): new insights from high-resolution CT scanning of the holotype. *Palaeontologia Electronica* 13, 1-16.
- S102. Gow, C.E. (1975). The morphology and relationships of *Youngina capensis* Broom and *Prolacerta broomi* Parrington. *Palaeontologia Africana* 18, 89-131.
- S103. Brusatte, S.L., Benton, M.J., Ruta, M., and Lloyd, G.T. (2008). Superiority, competition, and opportunism in the evolutionary radiation of dinosaurs. *Science* 321, 1485-1488.
- S104. Chatterjee, S. (1985). *Postosuchus*, a new thecodontian reptile from the Triassic of Texas and the origin of tyrannosaurs. *Philosophical Transactions of the Royal Society of London, Series B* 309, 395-460.
- S105. Flynn, J.J., Nesbitt, S.J., Parrish, J.M., Rianivoharimanana, L., and Wyss, A.R. (2010). A new species of *Azendohsaurus* (Diapsida: Archosauromorpha) from the Triassic Isalo Group of southwestern Madagascar: cranium and mandible. *Palaeontology* 53, 669-688.
- S106. Hunt, A.P. (1989). A new ?ornithischian dinosaur from the Bull Canyon Formation (Upper Triassic) of east-central New Mexico. In *Dawn of the Age of Dinosaurs in the American Southwest*, S.G. Lucas and A.P. Hunt, eds. (New Mexico Museum of Natural History), pp. 355-358, with two plates.
- S107. Nesbitt, S.J., and Norell, M.A. (2006). Extreme convergence in the body plans of an early suchian (Archosauria) and ornithomimid dinosaurs (Theropoda). *Proceedings of the Royal Society of London, Biological Sciences* 273, 1045-1048.
- S108. Sill, W.D. (1974). The anatomy of *Saurosuchus galilei* and the relationships of the rauisuchid thecodonts. *Bulletin of the Museum of Comparative Zoology* 146, 317-362.
- S109. Irmis, R.B., Parker, W.G., Nesbitt, S.J., and Liu, J. (2007). Early ornithischian dinosaurs: the Triassic record. *Historical Biology* 19, 3-22.
- S110. Nesbitt, S.J. (2007). The anatomy of *Effigia okeeffeae* (Archosauria, Suchia), theropod-like convergence, and the distribution of related taxa. *Bulletin of the American Museum of Natural History* 302, 1-84.
- S111. Brusatte, S.L., Benton, M.J., Ruta, M., and Lloyd, G.T. (2008). The first 50 Myr of dinosaur evolution: macroevolutionary pattern and morphological disparity. *Biology Letters* 4, 733-736.
- S112. Stayton, C.T. (2006). Testing hypotheses of convergence with multivariate data: morphological and functional convergence among herbivorous lizards. *Evolution* 60, 824-841.
- S113. Long, R.A., and Murry, P.A. (1995). Late Triassic (Carnian and Norian) tetrapods from the southwestern United States. *New Mexico Museum of Natural History & Science Bulletin* 4, 1-254.

- S114. Hunt, A.P. (1989). Cranial morphology and ecology among phytosaurs. In Dawn of the Age of Dinosaurs in the American Southwest, S.G. Lucas and A.P. Hunt, eds. (Albuquerque: New Mexico Museum of Natural History), pp. 349-354.
- S115. Stocker, M.R., and Butler, R.J. (2013). Phytosauria. In Anatomy, Phylogeny and Palaeobiology of Early Archosaurs and their Kin, S.J. Nesbitt, J.B. Desojo and R.B. Irmis, eds. (London: The Geological Society of London), pp. 91-117.
- S116. O'Leary, M.A., and Kaufman, S.G. (2012). MorphoBank 3.0: Web application for morphological phylogenetics and taxonomy. <http://www.morphobank.org>.
- S117. Hammer, Ø., Harper, D.A.T., and Ryan, P.D. (2001). PAST: Paleontological Statistics software package for education and data analysis. . *Paleontologia Electronica* 4, 1-9.
- S118. Legendre, P., and Legendre, L. (2012). Numerical Ecology, Third Edition, (Amsterdam: Elsevier).
- S119. Lloyd, G.T. (2015). Claddis: an R package for performing disparity and rate analysis on cladistic-type data sets. <https://github.com/graemetlloyd/Claddis>.
- S120. Oksanen, J., Blanchet, F.G., Kindt, R., Legendre, P., Minchin, P.R., B., O.H.R., Simpson, G.L., Solymos, P., Stevens, M.H.H., and Wagner, H. (2015). vegan: Community Ecology Package. URL <http://CRAN.R-project.org/package=vegan>. R package version 2.3-0.
- S121. Team, R.C. (2014). R: A language and environment for statistical computing. R Foundation for Statistical Computing. (Vienna, Austria: <http://www.R-project.org>).
- S122. Wills, M.A. (2001). Morphological disparity: a primer. In Fossils, Phylogeny, and Form: An Analytical Approach, J.M. Adrain, Edgecombe, G. D. and Lieberman, B. S., ed. (New York: Kluwer Academic/Plenum Publishers), pp. 55-144.
- S123. Gower, J.C. (1971). A general coefficient of similarity and some of its properties. *Biometrics* 27, 857-871.
- S124. Heckert, A.B., and Lucas, S.G. (1999). A new aetosaur (Reptilia: Archosauria) from the Upper Triassic of Texas and the phylogeny of aetosaurs. *Journal of Vertebrate Paleontology* 19, 50-68.
- S125. Sawin, H.J. (1947). The pseudosuchian reptile *Typothorax meadei*. *Journal of Paleontology* 21, 201-238.
- S126. Nesbitt, S.J., Irmis, R.B., Parker, W.G., Smith, N.D., Turner, A.H., and Rowe, T. (2009). Hindlimb osteology and distribution of basal dinosauromorphs from the Late Triassic of North America. *Journal of Vertebrate Paleontology* 29, 498-516.
- S127. Nesbitt, S.J., Sidor, C.A., Irmis, R.B., Angielczyk, K.D., Smith, R.M.H., and Tsuji, L.A. (2010). Ecologically distinct dinosaurian sister group shows early diversification of Ornithodira. *Nature* 464, 95-98.
- S128. Haubold, H., and Schaumberg, G. (1985). Die Fossilien des Kupferschiefers, (Lutherstadt Wittenberg: A. Ziemsen Verlag).
- S129. Rubidge, B.S. (2005). Re-uniting lost continents - fossil reptiles from the ancient Karoo and their wanderlust. *South African Journal of Geology* 108, 135-172.
- S130. Nesbitt, S.J., Stocker, M.R., Small, B.J., and Downs, A. (2009). The osteology and relationships of *Vancleavea campi* (Reptilia: Archosauriformes). *Zoological Journal of the Linnean Society* 157, 814-864.
- S131. Colbert, E.H. (1989). The Triassic dinosaur *Coelophysis*. *Museum of Northern Arizona Bulletin* 57, 1-160.
- S132. Sereno, P.C. (1991). Basal archosaurs: phylogenetic relationships and functional implications. *Society of Vertebrate Paleontology Memoir* 2, 1-53.
- S133. Dzik, J. (2003). A beaked herbivorous archosaur with dinosaur affinities from the early Late Triassic of Poland. *Journal of Vertebrate Paleontology* 23, 556-574.
- S134. Piechowski, R., and Dzik, J. (2010). The axial skeleton of *Silesaurus opolensis*. *Journal of Vertebrate Paleontology* 30, 1127-1141.
- S135. Irmis, R.B., Mundil, R., Martz, J.W., and Parker, W.G. (2011). High-resolution U-Pb ages from the Upper Triassic Chinle Formation (New Mexico, USA) support a diachronous rise of dinosaurs. *Earth and Planetary Science Letters* 309, 258-267.
- S136. Chatterjee, S. (1993). *Shuvosaurus*, a new theropod. *National Geographic Research & Exploration* 9, 274-285.
- S137. Stocker, M.R. (2010). Clarification of the skeletal anatomy of phytosaurs based on comparative anatomy and the most complete specimen of *Angistorhinus*. *Journal of Vertebrate Paleontology, Program and Abstracts* 2010, 170A.

- S138. Parker, W.G., Irmis, R.B., Nesbitt, S.J., Martz, J.W., and Browne, L.S. (2005). The Late Triassic pseudosuchian *Revueltosaurus callenderi* and its implications for the diversity of early ornithischian dinosaurs. *Proceedings of the Royal Society of London, Biological Sciences* 272, 963-969.
- S139. Ramezani, J., Hoke, G.D., Fastovsky, D.E., Bowring, S.A., Therrien, F., Dworkin, S.I., Atchley, S.C., and Nordt, L.C. (2011). High-precision U-Pb zircon geochronology of the Late Triassic Chinle Formation, Petrified Forest National Park (Arizona, USA): temporal constraints on the early evolution of dinosaurs. *Geological Society of America Bulletin* 123, 2142-2159.
- S140. Desojo, J.B., Heckert, A.B., Martz, J.W., Parker, W.G., Schoch, R.R., Small, B.J., and Sulej, T. (2013). Aetosauria: a clade of armoured pseudosuchians from the Upper Triassic continental beds. In *Anatomy, Phylogeny and Palaeobiology of Early Archosaurs and their Kin*, Volume 379, S.J. Nesbitt, J.B. Desojo and R.B. Irmis, eds. (London: The Geological Society of London), pp. 203-239.
- S141. Galton, P.M. (1977). On *Staurikosaurus pricei*, an early saurischian dinosaur from the Triassic of Brazil, with notes on the Herrerasauridae and Poposauridae. *Paläontologische Zeitschrift* 51, 234-245.
- S142. Colbert, E.H. (1961). The Triassic reptile *Poposaurus*. *Fieldiana* 14, 59-78.
- S143. Gauthier, J.A., Nesbitt, S.J., Schachner, E., Bever, G.S., and Joyce, W.G. (2011). The bipedal stem crocodylian *Poposaurus gracilis*: inferring function in fossils and innovation in archosaur locomotion. *Bulletin of the Peabody Museum of Natural History* 52, 107-126.
- S144. Parker, W.G., and Nesbitt, S.J. (2013). Cranial remains of *Poposaurus gracilis* (Pseudosuchia: Poposauroidae) from the Upper Triassic, the distribution of the taxon, and its implications for poposauroid evolution. In *Anatomy, Phylogeny and Palaeobiology of Early Archosaurs and their Kin*, Volume 379, S.J. Nesbitt, J.B. Desojo and R.B. Irmis, eds. (London: The Geological Society of London), pp. 503-523.
- S145. Weinbaum, J.C., and Hungerbühler, A. (2007). A revision of *Poposaurus gracilis* (Archosauria: Suchia) based on two new specimens from the Late Triassic of the southwestern U.S.A. *Paläontologische Zeitschrift* 81, 131-145.
- S146. Sereno, P.C., Forster, C.A., Rogers, R.R., and Monetta, A.M. (1993). Primitive dinosaur skeleton from Argentina and the early evolution of Dinosauria. *Nature* 361, 64-66.
- S147. Langer, M.C., and Benton, M.J. (2006). Early dinosaurs: A phylogenetic study. *Journal of Systematic Palaeontology* 4, 309-358.
- S148. Sereno, P.C., Martínez, R.N., and Alcober, O.A. (2013 (for 2012)). Osteology of *Eoraptor lunensis* (Dinosauria, Sauropodomorpha). *Journal of Vertebrate Paleontology* 32, 83-179.
- S149. Yates, A.M. (2003). The species taxonomy of the sauropodomorph dinosaurs from the Löwenstein Formation (Norian, Late Triassic) of Germany. *Palaeontology* 46, 317-337.
- S150. Moser, M. (2003). *Plateosaurus engelhardti* Meyer, 1837 (Dinosauria: Sauropodomorpha) aus dem Feuerletten (Mittelkeuper; Obertrias) von Bayern. *Zitteliana Reihe B* 24, 1-186.
- S151. Rowe, T.B., Sues, H.-D., and Reisz, R.R. (2011). Dispersal and diversity in the earliest North American sauropodomorph dinosaurs, with a description of a new taxon. *Proceedings of the Royal Society B: Biological Sciences* 278, 1044-1053.
- S152. Meyer, H.H.v. (1837). Mittheilungen, an Professor Bronn gerichtet. *Neues Jahrbuch für Mineralogie, Geologie und Paläontologie* 1837, 314-316.
- S153. Prieto-Márquez, A., and Norell, M.A. (2011). Redescription of a Nearly Complete Skull of *Plateosaurus* (Dinosauria: Sauropodomorpha) from the Late Triassic of Trossingen (Germany). *American Museum Novitates* 3727, 1-58.
- S154. Colbert, E.H., and Mook, C.C. (1951). The ancestral crocodylian *Protosuchus*. *Bulletin of the American Museum of Natural History* 97, 143-182.
- S155. Tanner, L.H., and Lucas, S.G. (2007). The Moenave Formation: Sedimentologic and stratigraphic context of the Triassic-Jurassic boundary in the Four Corners area, southwestern U.S.A. *Palaeogeography, Palaeoclimatology, Palaeoecology* 244, 111-125.
- S156. Clark, J.M. (1986). The relationships of the crocodylomorph archosaurs., Volume PhD Dissertation. (University of Chicago), p. 556.
- S157. Turner, A.H., and Sertich, J.J.W. (2010). Phylogenetic history of *Simosuchus clarki* (Crocodyliformes: Notosuchia) from the Late Cretaceous of Madagascar. *Society of Vertebrate Paleontology Memoir* 10, 177-236.

- S158. Tykoski, R.S., Rowe, T.B., Ketcham, R.A., and Colbert, M.W. (2002). *Calsoyasuchus valliceps*, a new crocodyliform from the Early Jurassic Kayenta Formation of Arizona. *Journal of Vertebrate Paleontology* 22, 593-611.
- S159. Pierce, S.E., and Benton, M.J. (2006). *Pelagosaurus typus* Bronn, 1841 (Mesoeucrocodylia: Thalattosuchia) from the Upper Lias (Toarcian, Lower Jurassic) of Somerset, England. *Journal of Vertebrate Paleontology* 26, 621-635.
- S160. Wilberg, E.W. (2015). What's in an outgroup? The impact of outgroup choice on the phylogenetic position of Thalattosuchia (Crocodylomorpha) and the origin of Crocodyliformes. *Systematic Biology*.
- S161. Butler, R.J. (2005). The 'fabrosaurid' ornithischian dinosaurs of the upper Elliot Formation (Lower Jurassic) of South Africa and Lesotho. *Zoological Journal of the Linnean Society* 145, 175-218.
- S162. Olsen, P.E., and Galton, P.M. (1984). A review of the reptile and amphibian assemblages from the Stormberg of southern Africa, with special emphasis on the footprints and the age of the Stormberg. *Palaeontologia Africana* 25, 87-110.
- S163. Galton, P.M. (1978). Fabrosauridae, the basal family of ornithischian dinosaurs (Reptilia: Ornithopoda). *Paläontologische Zeitschrift* 52, 138-159.
- S164. Butler, R.J., Upchurch, P., and Norman, D.B. (2008). The phylogeny of the ornithischian dinosaurs. *Journal of Systematic Palaeontology* 6, 1-40.
- S165. Xu, X., Clark, J.M., Mo, J., Choiniere, J., Forster, C.A., Erickson, G.M., Hone, D.W.E., Sullivan, C., Eberth, D.A., Nesbitt, S.J., et al. (2009). A Jurassic ceratosaur from China helps clarify avian digital homologies. *Nature* 459, 940-944.
- S166. Clark, J.M., Xu, X., Eberth, D.A., Forster, C.A., Malkus, M., Hemming, S., and Hernandez, R. (2006). The Middle-to-Late Jurassic terrestrial transition: New discoveries from the Shishugou Formation, Xinjiang, China. In *Ninth International Symposium on Mesozoic Terrestrial Ecosystems and Biota*. (Manchester, UK), pp. 26-28.
- S167. Marsh, O.C. (1877). Notice of new dinosaurian reptiles from the Jurassic formation. *The American Journal of Science and Arts* 14.
- S168. Foster, J. (2007). *Jurassic West: The Dinosaurs of the Morrison Formation and their World*, (Bloomington: Indiana University Press).
- S169. Madsen, J.H., Jr. (1976). *Allosaurus fragilis*: a revised osteology. *Utah Geological Survey Bulletin* 109, 1-163.
- S170. Turner, A.H., Pol, D., Clarke, J.A., Erickson, G.M., and Norell, M.A. (2007). A basal dromaeosaurid and size evolution preceding avian flight. *Science* 317, 1378-1381.
- S171. Charig, A.J., and Milner, A.C. (1986). *Baryonyx*, a remarkable new theropod dinosaur. *Nature* 324, 359-361.
- S172. Charig, A.J., and Milner, A.C. (1997). *Baryonyx walkeri*, a fish-eating dinosaur from the Wealden of Surrey. *Bulletin-Natural History Museum Geology Series* 53, 11-70.
- S173. Mateus, O., Araújo, R., Natário, C., and Castanheira, R. (2011). A new specimen of the theropod dinosaur *Baryonyx* from the early Cretaceous of Portugal and taxonomic validity of *Suchosaurus*. *Zootaxa* 2827, 54-68.
- S174. Rayfield, E.J., Milner, A.C., Xuan, V.B., and Young, P.G. (2007). Functional morphology of spinosaur 'crocodile-mimic' dinosaurs. *Journal of Vertebrate Paleontology* 27, 892-901.
- S175. Dal Sasso, C., Maganuco, S., Buffetaut, E., and Mendez, M.A. (2005). New information on the skull of the enigmatic theropod *Spinosaurus*, with remarks on its size and affinities. *Journal of Vertebrate Paleontology* 25, 888-896.
- S176. Smith, J.B., Lamanna, M.C., Mayr, H., and Lacovara, K.J. (2006). New information regarding the holotype of *Spinosaurus aegyptiacus* Stromer, 1915. *Journal of Paleontology* 80, 400-406.
- S177. Stromer, E. (1915). Ergebnisse der Forschungsreisen Prof. E. Stromers in den Wüsten Ägyptens. II. Wirbeltier-Reste der Baharije-Stufe (unterstes Cenoman) 3. Das Original des Theropoden *Spinosaurus aegyptiacus* nov. gen., nov. spec. *Abhandlungen der Königlich Bayerischen Akademie der Wissenschaften Mathematisch - Physikalische Klasse* 28, 1-32.
- S178. Ibrahim, N., Sereno, P.C., Dal Sasso, C., Maganuco, S., Fabbri, M., Martill, D.M., Zouhri, S., Myhrvold, N., and Iurino, D.A. (2014). Semiaquatic adaptations in a giant predatory dinosaur. *Science* 345, 1613-1616.

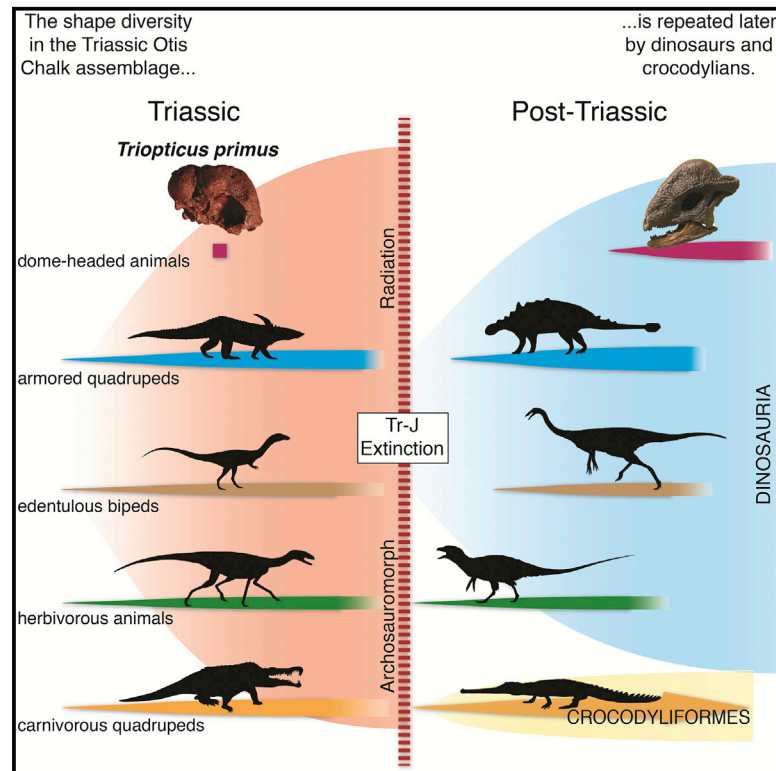
- S179. Sereno, P.C., Beck, A.L., Dutheil, D.B., Gado, B., Larsson, H.C.E., Lyon, G.H., Marcot, J.D., Rauhut, O.W.M., Sadleir, R.W., Sidor, C.A., et al. (1998). A long-snouted predatory dinosaur from Africa and the evolution of spinosaurids. *Science* 282, 1298-1302.
- S180. Makovicky, P.J., Kobayashi, Y., and Currie, P.J. (2004). Ornithomimosauria. In *The Dinosauria*, second edition, D.B. Weishampel, P. Dodson and H. Osmólska, eds. (Berkeley: University of California Press), pp. 137-150.
- S181. Eberth, D.A., Thomas, R.G., and Deino, A.L. (1992). Preliminary K-Ar dates from bentonites in the Judith River and Bearpaw formations (Upper Cretaceous) of Dinosaur Provincial Park, southern Alberta, Canada. In *Aspects of Nonmarine Cretaceous Geology*, N.J. Mateer and P.J. Chen, eds. (Beijing: China Ocean Press), pp. 296-304.
- S182. Norell, M.A., Makovicky, P.J., and Currie, P.J. (2001). The beaks of ostrich dinosaurs. *Nature* 412, 873-874.
- S183. Tahara, R., and Larsson, H.C.E. (2011). Cranial pneumatic anatomy of *Ornithomimus edmontonicus* (Ornithomimidae: Theropoda). *Journal of Vertebrate Paleontology* 31, 127-143.
- S184. Sullivan, R.M. (2003). Revision of the dinosaur *Stegoceras* Lambe (Ornithischia, Pachycephalosauridae). *Journal of Vertebrate Paleontology* 23, 181-207.
- S185. Eberth, D.A., and Hamblin, A.P. (1993). Tectonic, stratigraphic, and sedimentological significance of a regional discontinuity in the upper Judith River Group (Belly River wedge) of southern Alberta, Saskatchewan, and northern Montana. *Canadian Journal of Earth Science* 30, 174-200.
- S186. Sues, H.-D., and Galton, P.M. (1987). Anatomy and classification of the North America Pachycephalosauria (Dinosauria: Ornithischia). *Palaeontographica Abt. A* 198, 1-40.
- S187. Kirkland, J.I. (1998). A polacanthine ankylosaur (Ornithischia: Dinosauria) from the Early Cretaceous (Barremian) of eastern Utah. *New Mexico Museum of Natural History and Science Bulletin* 14, 271-281.
- S188. Carpenter, K., and Kirkland, J.I. (1998). Review of Lower and Middle Cretaceous ankylosaurs from North America. *New Mexico Museum of Natural History and Science Bulletin* 14, 249-269.
- S189. Ostrom, J.H. (1970). Stratigraphy and paleontology of the Cloverly Formation (Lower Cretaceous) of the Bighorn Basin area, Wyoming and Montana. *Peabody Museum of Natural History Bulletin* 35, 1-234.
- S190. Oppel, M. (1811). *Die Ordnungen, Familien, und Gattungen der Reptilien als Prodrum einer Naturgeschichte derselben.*, (Munich: Joseph Lindauer).
- S191. Brochu, C.A. (2003). Phylogenetic approaches toward crocodylian history. *Annual Review of Earth and Planetary Sciences* 31, 357-397.
- S192. Benton, M.J. (1999). *Scleromochlus taylori* and the origin of dinosaurs and pterosaurs. *Philosophical Transactions of the Royal Society of London, Series B* 354, 1423-1446.
- S193. Juul, L. (1994). The phylogeny of basal archosaurs. *Palaeontologia Africana* 31, 1-38.
- S194. Novas, F.E. (1996). Dinosaur monophyly. *Journal of Vertebrate Paleontology* 16, 723-741.
- S195. Sereno, P.C., and Novas, F.E. (1994). The skull and neck of the basal theropod *Herrerasaurus ischigualastensis*. *Journal of Vertebrate Paleontology* 13, 451-476.
- S196. Sereno, P.C. (2000). The fossil record, systematics and evolution of pachycephalosaurs and ceratopsians from Asia. In *The Age of Dinosaurs in Russia and Mongolia*, M.J. Benton, M.A. Shishkin, D.M. Unwin and E.N. Kurochkin, eds. (Cambridge: Cambridge University Press), pp. 480-516.
- S197. Maryńska, T., Chapman, R.E., and Weishampel, D.B. (2004). Pachycephalosauria. In *The Dinosauria* (2nd Edition), D.B. Weishampel, P. Dodson and H. Osmólska, eds. (Berkeley: University of California Press), pp. 464-477.
- S198. Gauthier, J. (1986). Saurischian monophyly and the origin of birds. *Memoirs of the California Academy of Sciences* 8, 1-55.
- S199. Parrish, J.M. (1993). Phylogeny of the Crocodylotarsi, with reference to archosaurian and crurotarsan monophyly. *Journal of Vertebrate Paleontology* 13, 287-308.
- S200. Gauthier, J., Kluge, A.G., and Rowe, T. (1988). Amniote phylogeny and the importance of fossils. *Cladistics* 4, 105-209.
- S201. Hungerbühler, A. (2002). The Late Triassic phytosaur *Mystriosuchus westphali*, with a revision of the genus. *Palaeontology* 45, 377-418.

- S202. Gower, D.J., and Sennikov, A.G. (1997). *Sarmatosuchus* and the early history of the Archosauria. *Journal of Vertebrate Paleontology* 17, 60-73.
- S203. Stocker, M.R. (2010). A new taxon of phytosaur (Archosauria: Pseudosuchia) from the Late Triassic (Norian) Sonsela Member (Chinle Formation) in Arizona, and a critical reevaluation of *Leptosuchus* Case 1922. *Palaeontology* 53, 997-1022.
- S204. Sereno, P.C. (1986). Phylogeny of the bird-hipped dinosaurs (Order Ornithischia). *National Geographic Research* 2, 234-256.
- S205. Nesbitt, S.J. (2009). The early evolution of archosaurs: relationships and the origin of major clades. (New York: Columbia University), p. 665.
- S206. Bennett, S.C. (1996). The phylogenetic position of the Pterosauria within Archosauromorpha. *Zoological Journal of the Linnean Society* 118, 261-308.
- S207. Gauthier, J.A. (1984). A cladistic analysis of the higher systematic categories of the Diapsida. (Berkeley: University of California, Berkeley), p. 564.
- S208. Shepard, R.N. (1962). The analysis of proximities: multidimensional scaling with an unknown distance function. *Psychometrika* 27, 125-139.

Current Biology

A Dome-Headed Stem Archosaur Exemplifies Convergence among Dinosaurs and Their Distant Relatives

Graphical Abstract



Authors

Michelle R. Stocker, Sterling J. Nesbitt, Katharine E. Criswell, ..., Timothy B. Rowe, Ryan Ridgely, Matthew A. Brown

Correspondence

stockerm@vt.edu

In Brief

Stocker et al. describe *Triopticus primus*, a bizarre Late Triassic animal, whose skull structure is converged on by distantly related pachycephalosaur dinosaurs. The unique body plans observed in *Triopticus* and other archosaurs at the “dawn of the age of dinosaurs” re-evolved in dinosaurs and crocodylians after the end-Triassic mass extinction.

Highlights

- Cretaceous-aged dome-headed dinosaurs are convergent with Triassic-aged *Triopticus*
- Archosauromorph reptiles evolved extreme body plans after the end-Permian extinction
- Dinosaurs repeated body plans present in their Triassic-aged relatives
- The early evolution of body plans may constrain later body plans in the same group

